Project Report
ATC-450

Radar Coverage Analysis for the Terminal Precipitation on the Glass Program

J.Y.N. Cho
W.J. Dupree

4 March 2022

Lincoln Laboratory
MASSACHUSETTS INSTITUTE OF TECHNOLOGY
LEXINGTON, MASSACHUSETTS

This report is the result of studies performed at Lincoln Laboratory, a federally funded research and development center operated by Massachusetts Institute of Technology. This material is based upon work supported by the Federal Aviation Administration under Air Force Contract No. FA8702-15-D-0001. Any opinions, findings, conclusions or recommendations expressed in this material are those of the author(s) and do not necessarily reflect the views of the Federal Aviation Administration.

TECHNICAL REPORT STANDARD TITLE PAGE

1. Report No.	2. Government Accession No.	3. Recipient's Catalog No.
ATC-450		

4. Title and Subtitle	5. Report Date
Radar Coverage Analysis for the Terminal Precipitation on the Glass Program	4 March 2022
	6. Performing Organization Code

7. Author(s)	8. Performing Organization Report No.
J.Y.N. Cho, W.J. Dupree	ATC-450

9. Performing Organization Name and Address	10. Work Unit No. (TRAIS)
MIT Lincoln Laboratory 244 Wood Street Lexington, MA 02421	11. Contract or Grant No. FA8702-15-D-0001

12. Sponsoring Agency Name and Address	13. Type of Report and Period Covered
Department of Transportation Federal Aviation Administration 800 Independence Ave., S.W. Washington, DC 20591	Project Report
	14. Sponsoring Agency Code

15. Supplementary Notes

This report is based on studies performed at Lincoln Laboratory, a federally funded research and development center operated by Massachusetts Institute of Technology, under Air Force Contract FA8702-15-D-0001.

16. Abstract

The Terminal Precipitation on the Glass (TPoG) program proposes to improve the STARS precipitation depiction by adding an alternative precipitation product based on a national weather-radar-based mosaic, i.e., the NextGen Weather System (aka NextGen Weather Processor [NWP] and Common Support Services Weather [CSS-Wx]). This report describes spatial and temporal domain analyses conducted over the 146 terminal radar approach control (TRACON) airspaces that are within scope of TPoG to identify and quantify future TPoG benefits, as well as potential operational issues.

17. Key Words	18. Distribution Statement
	DISTRIBUTION STATEMENT A. Approved for public release: distribution unlimited.

19. Security Classif. (of this report)	20. Security Classif. (of this page)	21. No. of Pages	22. Price
Unclassified	Unclassified	104	

FORM DOT F 1700.7 (8-72) Reproduction of completed page authorized

This page intentionally left blank.

EXECUTIVE SUMMARY

In a previous study, five shortfall areas were identified in the operational usage of the current standard terminal automation replacement system (STARS) precipitation display:

1. Insufficient accuracy in depicting precipitation event in relevant airspace.
2. Insufficient capability to identify and remove false precipitation depiction in relevant airspace.
3. Insufficient consistency of precipitation event depictions in relevant airspace.
4. Insufficient coverage of precipitation event depiction in relevant airspace.
5. Insufficient availability of precipitation event depiction in relevant airspace.

The Terminal Precipitation on the Glass (TPoG) program proposes to improve the STARS precipitation depiction by adding an alternative precipitation product based on a national weather-radar-based mosaic, i.e., the NextGen Weather System (aka NextGen Weather Processor [NWP] and Common Support Services Weather [CSS-Wx]). This report describes spatial and temporal domain analyses conducted over the 146 terminal radar approach control (TRACON) airspaces that are within scope of TPoG to identify and quantify future TPoG benefits, as well as potential operational issues. The main conclusions are as follows:

- The addition of TPoG would increase the median (over all TRACONs) weather-weighted three-dimensional (3D) coverage from 96.4% to 98.4%. For a more focused airspace within 6 NM of the airport towers equipped with STARS inside the TRACONs, the improvement is from 90.5% to 99.0%. These enhancements address shortfall #4 (insufficient coverage).
- The weather radar data ingested by the NextGen Weather System provide superior horizontal resolution compared to the airport surveillance radar (ASR) data. The median limiting horizontal resolution (the larger of range or azimuthal resolution) taken over all TRACONs is 4.0 km for ASRs and 1.2 km for weather radars. Within 6 NM of the airport towers, this improvement is from 2.8 km to 0.89 km. Although the final precipitation product display resolution will be limited by the NextGen Weather System grid spacing of 1 km and, potentially, the chosen processing scheme employed in the TPoG adaptor, a significant degree of horizontal resolution enhancement can be expected in many TRACONs with TPoG. This may help address shortfall #1 (insufficient accuracy), if coarse horizontal resolution is one of the causes behind the perceived inaccuracy of STARS precipitation depiction.
- The increase in overlapping radar coverage with TPoG will correspondingly raise the aggregate precipitation product availability on STARS. Without TPoG, only 22% of TRACONs have an average radar coverage overlap of two or more radars; this increases to 100% with the addition of TPoG. This helps to address shortfall #5 (insufficient availability).

- Because of the highly overlapping nature of weather radar coverage, TPoG would receive multiple radar data updates within the 25-second NextGen Weather System product update period in most TRACONs. This implies that the 25-second period represents a meaningful refresh of the airspace observations.
- Specific TRACONs were identified where weather radar coverage might be insufficient for operational usage. These are (with mean 3D coverage in parentheses): Eugene, OR (56% with Medford, OR airspace included, 38% without); Moses Lake, WA (57%); Roswell, NM (67%), Casper, WY (65%), and Bangor, ME (71%). Further evaluation involving real data and operational air traffic control personnel is recommended.
- Estimated latency for TPoG from start of radar observation to arrival of the precipitation product at the STARS display input is comparable to that of the current ASR-based precipitation product. This conclusion is based on a particular posited TPoG architecture (the actual operational architecture is yet to be determined), and assumes that NextGen Weather System's motion compensation technique is effective in eliminating location errors; it excludes situations of very rapid growth or decay in convective storms.

Although not specifically analyzed in this study, the proposed TPoG solution also helps to address shortfall #2 (insufficient capability to identify and remove false precipitation) due to the weather radars' superior data quality and NextGen Weather System's multi-sensor techniques for anomaly removal. Furthermore, the national mosaic nature of the NextGen Weather System helps to address shortfall #3 (insufficient consistency), since the same precipitation product source would be used to generate the STARS displays in neighboring TRACONs. Therefore, operational implementation and deployment of TPoG should help address all five of the identified STARS precipitation display shortfall areas. Note, however, that this is only a theoretical analysis. It is recommended that the results presented here be used to guide further evaluations of TPoG performance under simulated operational settings.

TABLE OF CONTENTS

This page intentionally left blank.

LIST OF ILLUSTRATIONS

LIST OF TABLES

This page intentionally left blank.

1. INTRODUCTION

Safe and efficient air traffic control (ATC) requires timely and accurate monitoring of weather. Such observations are provided by a combination of in situ and remote sensing instruments located on the ground, onboard aircraft, and on satellites. For airport and terminal radar approach control (TRACON) airspaces with coverage from airport surveillance radars (ASRs), real-time precipitation mapping is primarily provided by the six-level video integrator and processor (VIP) reflectivity field produced by the ASRs. This product is displayed as a simultaneous overlay on aircraft tracks shown on the standard terminal automation replacement system (STARS), which helps controllers to route air traffic within their domains.

It has been noted, however, that airport tower and TRACON controllers do not always have access to accurate, reliable, and timely depictions of precipitation. Subpar precipitation characterization reduces the controller's ability to issue accurate weather advisories in terminal airspace, to effectively maneuver aircraft around hazardous storms cells, and to effectively anticipate traffic pattern changes and devise aircraft separation strategies. In response to these concerns, the Federal Aviation Administration (FAA) launched a concept maturity and technology demonstration (CMTD) activity, the Terminal Precipitation on the Glass (TPoG) program, to determine whether alternative precipitation data sources and dissemination mechanisms would be viable and beneficial for national airspace (NAS) operations. One of the initial TPoG tasks was an analysis of STARS precipitation display shortfalls. Five specific areas were identified (FAA 2020a):

1. Insufficient accuracy in depicting precipitation event in relevant airspace.
2. Insufficient capability to identify and remove false precipitation depiction in relevant airspace.
3. Insufficient consistency of precipitation event depictions in relevant airspace.
4. Insufficient coverage of precipitation event depiction in relevant airspace.
5. Insufficient availability of precipitation event depiction in relevant airspace.

TPoG proposes to improve the STARS precipitation depiction by integrating alternative radar-based weather data (2020b). Various alternatives were considered, including the post-processing of ASR data and local weather processors such as the Integrated Terminal Weather System (ITWS); the preferred solution was one based on a national weather radar mosaic (FAA 2020c), i.e., the NextGen Weather System.

On average, national weather radar mosaic data should provide a number of advantages over local ASR data, such as consistent weather depiction across neighboring terminal and en route domains, as well as better elimination of artifacts due to multi-radar viewing angles and advanced processing techniques. However, there may be particular TRACONs that do not have weather radars that are close enough (or blocked by terrain) to provide the needed coverage. There are also uncertainties regarding issues of weather

radar data availability, update period, and latency. This report aims to address these concerns as well as identify potential benefits.

The scope of this study encompasses the 146 TRACONs (Figure 1-1) associated with the TPoG program. As this study supports a future-oriented program, the radar associations are not aligned to the current state, but to the planned configuration after the completion of the ongoing ASR divestiture program (https://www.faa.gov/air_traffic/technology/radardivestiture/). Also, Peoria (PIA) and Springfield, IL (SPI) were incorporated as remote towers under St. Louis (T75) per future plans.

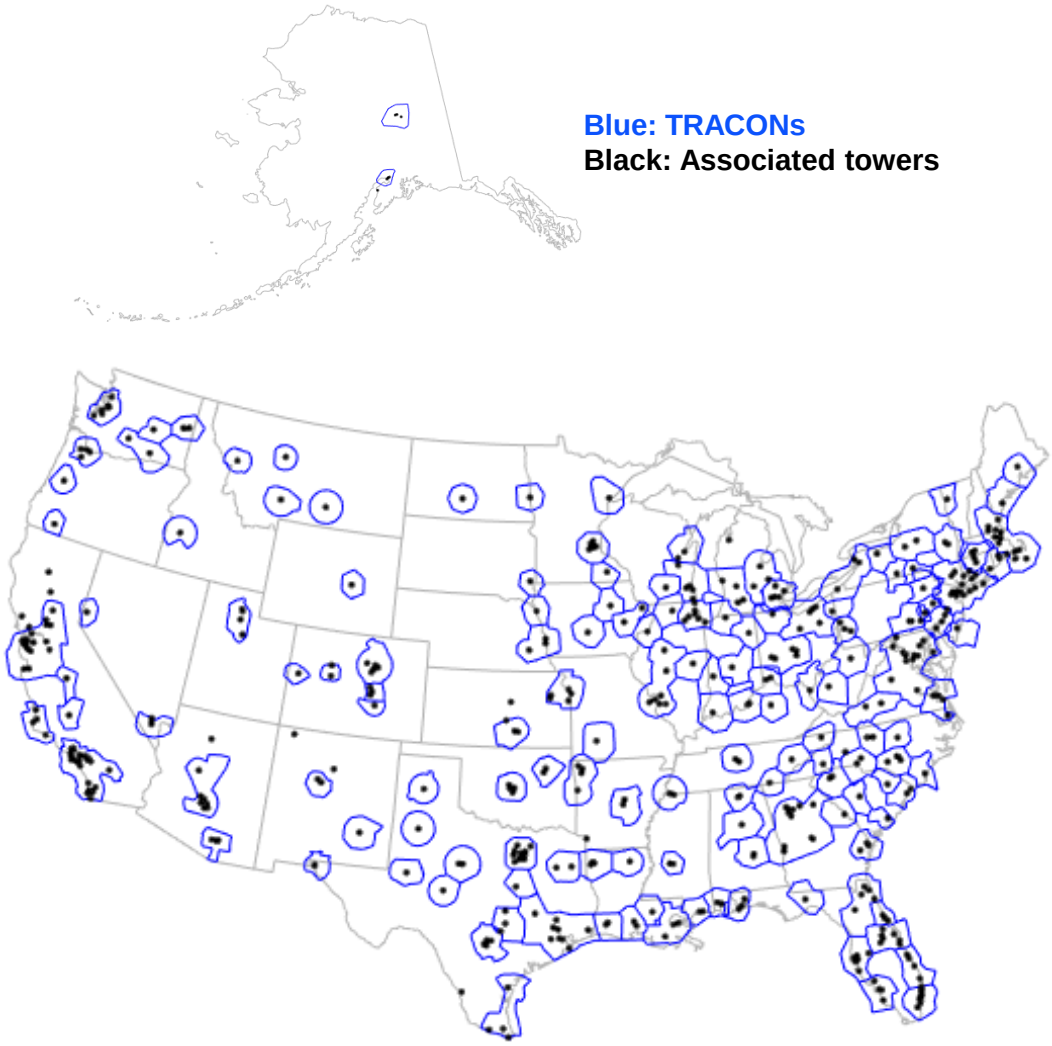

Figure 1-1. TRACONs included in this study.

Individual TRACON listings are provided in Appendix A. Table A-1 shows the TRACONs and the ASRs/GPNs that feed STARS at each site. (GPN, or ground position navigation, radar is the military equivalent of the ASR: GPN-20 = ASR-8, GPN-27 = ASR-9, and GPN-30 = ASR-11.) Figure 1-2 shows the ASR locations, and Table A-2 provides the locations and owner agencies of the ASRs. Table A-3 lists the TRACONs and their associated towers. Five of the 146 TRACONs have control responsibility over secondary airspaces that are physically separated from the primary TRACON boundary, with STARS displays at the secondary airspace towers that are "slaved" off of the primary STARS. These secondary airspaces are listed in Table A-1 separately after the 146 TRACONs, with the primary TRACON affiliation shown in parentheses. Unless otherwise noted, the results for those five TRACONs will include those of the associated secondary airspaces.

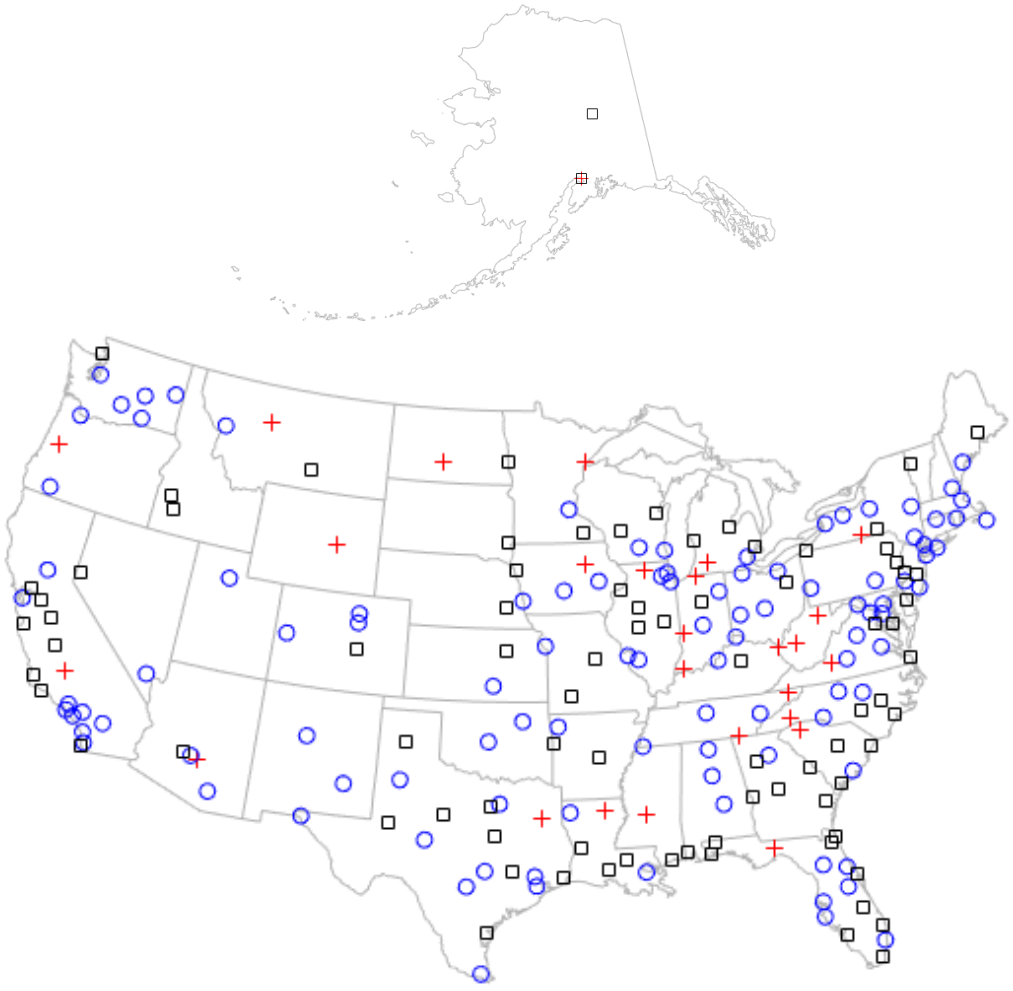

Figure 1-2. Locations of ASRs included in this study: ASR-8 (red cross), ASR-9 (blue circle), and ASR-11 (black square).

The precipitation product available on the STARS displays is primarily based on data from ASRs. Air Route Surveillance Radar-4 (ARSR-4) precipitation data is also supplied to some STARS sites, but is rarely used (Worris and Cho 2018). Common Air Route Surveillance Radar (CARSR) precipitation data is currently only generated for STARS displays in the Phoenix (P50) TRACON, where there is a gap in ASR coverage in the northern sector (Worris and Cho 2018). The long-range radar precipitation products have various data quality and resolution issues (Carmouche 2012) that make them sub-optimal for terminal airspace usage. For these reasons, we limited the scope in our study to the comparison between ASR and weather radar coverages.

Aside from the spatial and temporal coverage and resolution issues that were studied for this report, note that there are underlying data quality differences in the radar data that feed into the precipitation products. Because the ASRs were designed primarily for aircraft detection and tracking, and not specifically for meteorological observations, their weather data quality is decidedly inferior to the output quality of weather radars. This can be seen even in the radar specifications. For example, the ASR-11 specification allows for a maximum weather reflectivity error (in the absence of clutter) of 2.5 dB (Raytheon 1999), whereas for the Next Generation Weather Radar (NEXRAD) this specification is only 1 dB (ROC 2008). The weather radars included in this study all have lower reflectivity estimate errors, narrower antenna beamwidths (better angular resolution at a given range), lower antenna sidelobes (less out-of-resolution-volume contamination), higher sensitivity, and better clutter filtering capability compared to the ASRs. See, for example, Chapter 7 of Mahapatra (1999) for further discussion on this topic. Therefore, on the basis of superior data quality, the use of weather radar data to generate a precipitation product for STARS should help address shortfalls #1 (accuracy) and #2 (false precipitation).

Even with these inherent data quality advantages, mosaics generated from weather radar data may not necessarily be operationally acceptable at every TRACON and airport. To reiterate, that is because the locations of the weather radars may be too far or obstructed by terrain to provide adequate coverage and/or spatial resolution. Section 2 addresses these issues.

There are also potential time-domain issues that need to be investigated. Would the data latency and effective update rates of a national weather radar mosaic be fast enough to be acceptable for terminal ATC operational usage? Would the data availability rate meet the requirements of terminal ATC operations? These questions are analyzed in Section 3.

2. SPATIAL DOMAIN ANALYSES

The future operational NextGen Weather System will ingest radar data from NEXRADs (ROC 2008), Terminal Doppler Weather Radars (TDWRs; FAA 1995), and Canadian weather radars (CANRADs; Sills and Joe 2019). All of these radars will collectively be referred to as weather (WX) radars in this report, and will be the subject of our analyses. Figure 2-1 shows the locations of the WX radars.

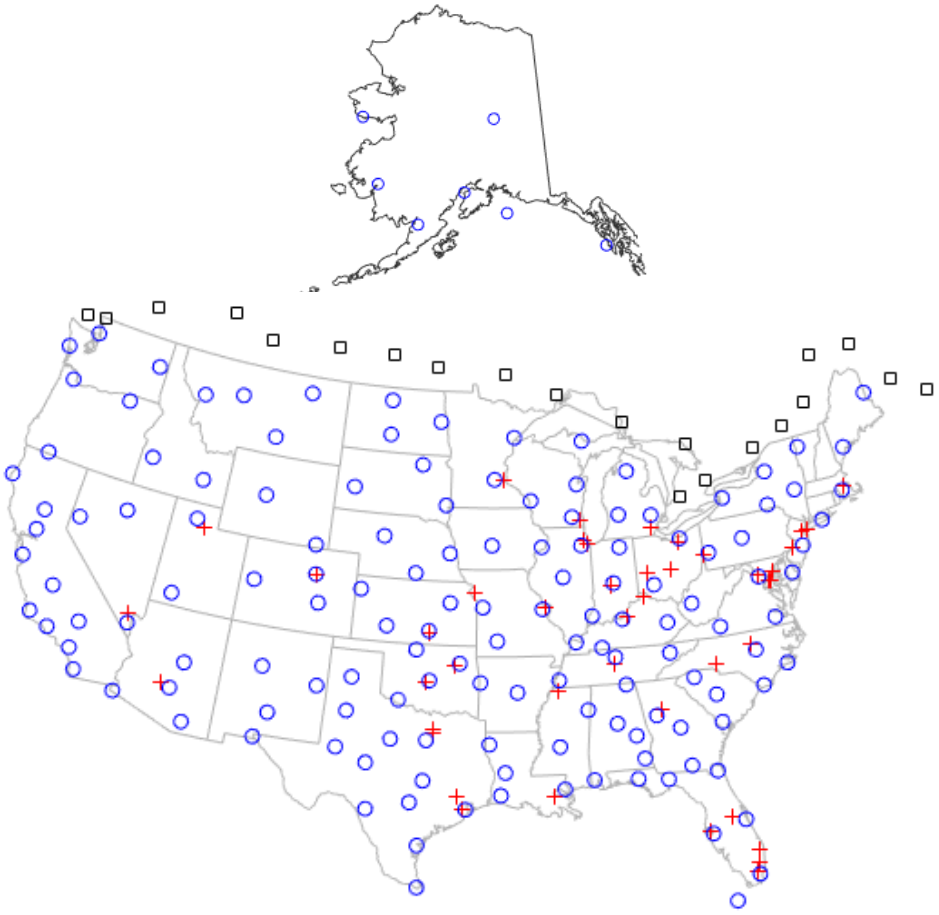

Figure 2-1. NEXRAD (blue circle), TDWR (red cross), and CANRAD (black square) locations.

The spatial domain metrics of interest in assessing the viability and suitability of a precipitation product in a particular airspace are 3D coverage and horizontal resolution. The two-dimensional (2D) horizontal precipitation products of interest here—0–60-kft composite reflectivity (CR) and vertically integrated liquid (VIL) water—do not have vertical resolution. Analysis results for the two metrics are given in the following two sections.

2.1 3D COVERAGE

Horizontal weather radar coverage is determined by the minimum and maximum range of observation. Sensitivity is not an issue for this study, because all of the radars have sufficient sensitivity to detect the lowest level of reflectivity (18 dBZ) needed to delineate Level 1 of the six-level VIP product throughout their instrumented ranges. Vertical weather radar coverage is set by the minimum and maximum elevation angles of the antenna beam, minus and plus half the elevation beam width. Table 2-1 lists the corresponding values of these parameters for the different radar types.

Table 2-1

Radar Characteristics Relevant for Coverage

Parameter	NEXRAD	TDWR	CANRAD	ASR/GPN
Minimum Observation Range	1 km	0.3 km	0.5 km	0.93 km
Maximum Observation Range	460 km	90 km*	245 km	111 km
Minimum Elevation Angle	0.5° (with exceptions)	Site dependent	0.4°	N/A
Maximum Elevation Angle	19.5°	Site dependent	24.4°	N/A
Elevation Beam Width	1°	0.6°	0.9°	N/A

*TDWR has one 460-km reflectivity scan per volume, but NextGen Weather System clips the range to 90 km during mosaicking.

Although NEXRAD maximum elevation angles are fixed at 19.5°, and most sites have a minimum elevation angle of 0.5°, there is a small subset of locations with lower minimum elevation angles, mostly at high-altitude sites to improve surrounding low-altitude coverage. These exceptions are listed in Appendix A, Table A-4. For TDWR, the minimum and maximum elevation angles are customized to optimize low-altitude wind shear detection over the associated airports. These values are listed in Appendix A, Table A-5. These site-adjustable parameters could change in the future, but since we have no way of knowing what changes there may be, we used the current values for our study.

Calculating the coverage of the ASRs is more complicated. First, their antenna beams are not symmetrically shaped in the elevation angle dimension, so the actual patterns are used to estimate the elevation coverage with respect to range. Second, they utilize a low beam for transmit, and a combination of the low beam (at closer ranges) and a high beam (at farther ranges) on receive (Figure 2-2). This is done in order to manage the trade-off between ground clutter and low-altitude coverage at close range. Each of the ASR types (ASR-8, -9, and -11) employ somewhat different techniques for this beam combination on

receive (IE 2019; FAA 2008; FAA 2019). Furthermore, the transition range from high beam to low beam can be tailored at each site (and can even be azimuthally dependent). This fine-grained data is not tracked in a national database, and requesting the data from each site was deemed to be an unreasonably time-consuming task for this project. Therefore, we used the default values for the beam transition range of 13 NM (ASR-8), 15 NM (ASR-9 without Weather Systems Processor (WSP)), 3.75 NM (ASR-9 with WSP), and 6.5 NM (ASR-11).

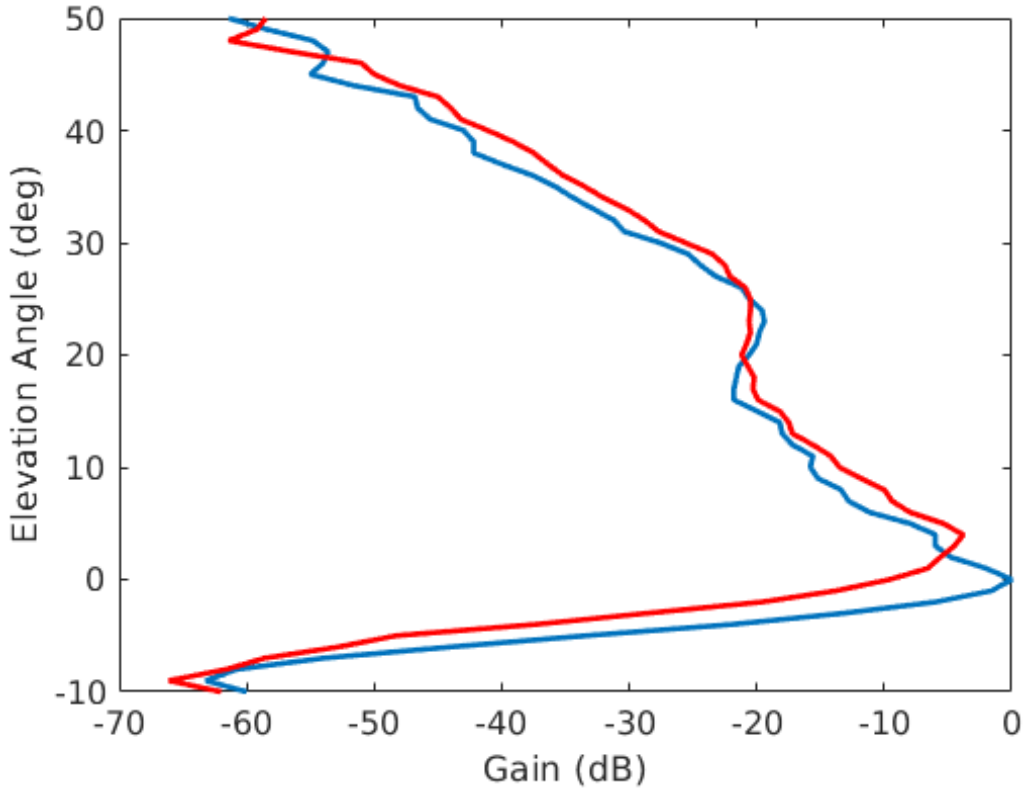

Figure 2-2. ASR two-way elevation angle antenna patterns. Blue is transmit and receive on low beam, red is transmit on low beam and receive on high beam.

Although the antenna beam patterns of all ASR types are essentially the same, the elevation angle mechanical tilt of the antenna reflector is site-adjustable. Again, this location-specific information was not available in a national database, so we assumed the default angle (2°) at all sites. This means that the two-way beam patterns in Figure 2-2 are shifted up by 2°.

The 3D coverage calculation must also account for ground obstructions. For this purpose, we used the Shuttle Radar Tomography Mission (SRTM) Level 2 (1 arcsec) data. We chose this digital elevation data because it includes structures on top of the Earth's terrain. In areas where Level 2 was not available (e.g., Alaska) we used the Level 1 (3 arcsec) SRTM data. Beam propagation geometry assumed a standard 4/3-Earth-radius model to account for atmospheric refraction (e.g., Skolnik, 2008). Radar coverage was computed at 1/1200-deg (lat/lon) horizontal spacing and variable vertical resolution (25 m for 0–3000 m MSL, 50 m for 3050–4000 m MSL, 100 m for 4100–6000 m MSL, 200 m for 6200–9000 m, and 400 m for 9400–15,000 m MSL). The coverage calculation procedure was similar to previous studies (e.g., Cho 2015).

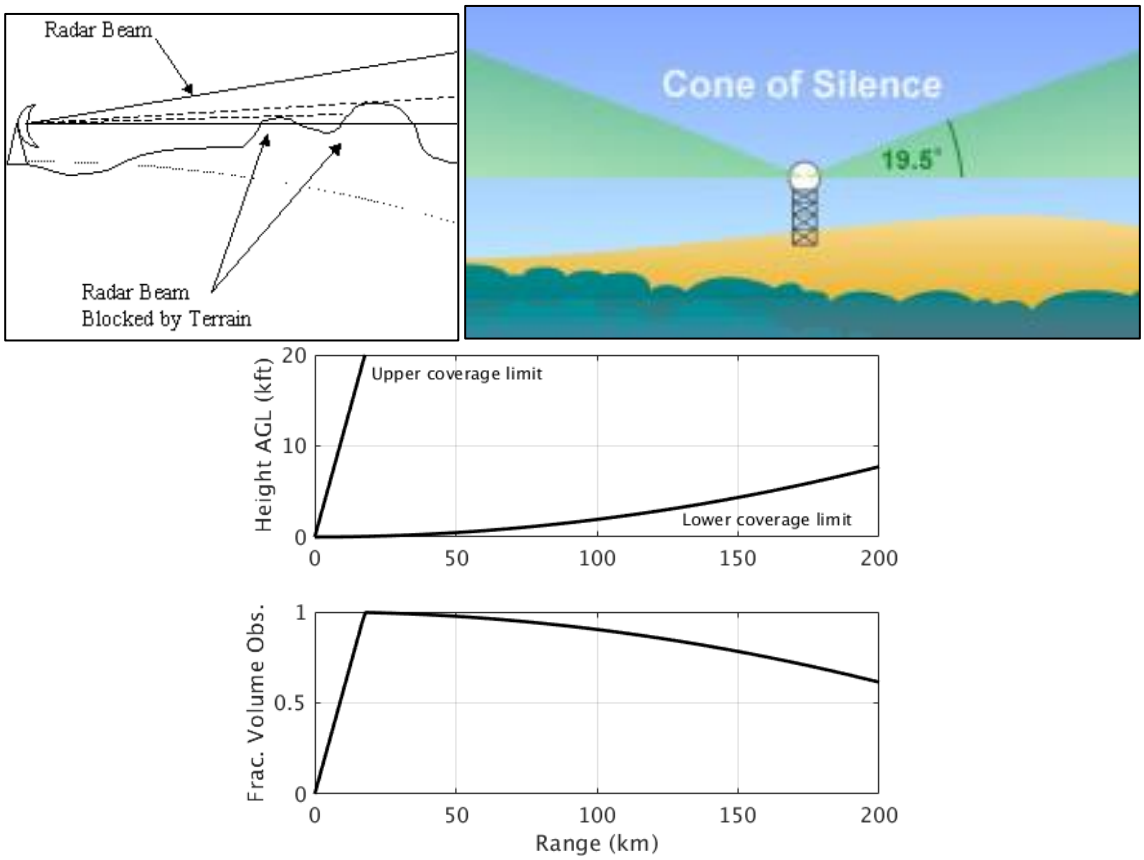

Figure 2-3. Illustrations of radar beam blockage by terrain (top left), NEXRAD cone of silence (top right), height above ground level (AGL) coverage limits (center), and FVO example for NEXRAD with a smooth Earth and a ceiling of 20 kft (bottom).

All of these input data discussed so far allow us to determine if any given point in 3D space is observed by a particular radar. It would be more convenient and useful, however, to have a metric that summarized the degree of vertical coverage in order to map that quantity in 2D space. To this end, we defined a quantity called the fraction of vertical volume observed (FVO) in an earlier unrelated study (Cho and Kurdzo 2019). FVO is the fraction of a vertical column observable by a radar, with the ground as the floor and a specified altitude as the ceiling. It includes the effects of the Earth's curvature, ground structure blockage, and the radar's cone of silence (the space above its maximum antenna beam elevation angle that it cannot observe) in one metric (Figure 2-3).

FVO treats all altitudes equally and has a hard cut-off (ceiling). Weather, however, does not occur equally at all altitudes, and does not cease abruptly at a certain height. Thus, in order to have a metric that takes into account the actual probability of operationally significant weather occurrence, we extended the FVO concept to include altitude-dependent weather occurrence weighting. This new metric, dubbed the weighted FVO, or WFVO, integrates local weather characteristics with radar coverage.

To compute WFVO, we needed the vertical profiles of radar echo occurrence for each TRACON. To derive this information, we first compiled vertical histograms of the NextGen Weather System's Level 2 or greater, i.e., reflectivities of 30 dBZ or greater, over each latitude-longitude grid cell. Level 2 was chosen, because it was perceived to be the lowest precipitation level for ATC operational concerns. 542 days of relatively active weather days over 2019-2021 were used for this compilation. Only areas with excellent radar coverage (FVO > 0.98, with a ceiling of 70 kft) were kept, because otherwise the data would be biased by missing low altitude coverage, terrain blockage, and radar cones of silence (Figure 2-4). This filtered "key hole" histogram data were aggregated inside local regions as defined by closest distance to a NEXRAD (Figure 2-5). Finally, histograms of Level 2+ weather occurrence were computed for each TRACON by computing distance-weighted means of the NEXRAD-location-associated regional histograms; a 2D Gaussian kernel with a width of 200 km was employed for the distance weighting. For the Alaskan TRACONs, we used the S46 (Seattle, WA) profile as the closest proxy.

Figure 2-4. Areas with WX radar FVO > 0.98 shown in black. Only these areas were used to compute the vertical histograms of Level 2+ weather.

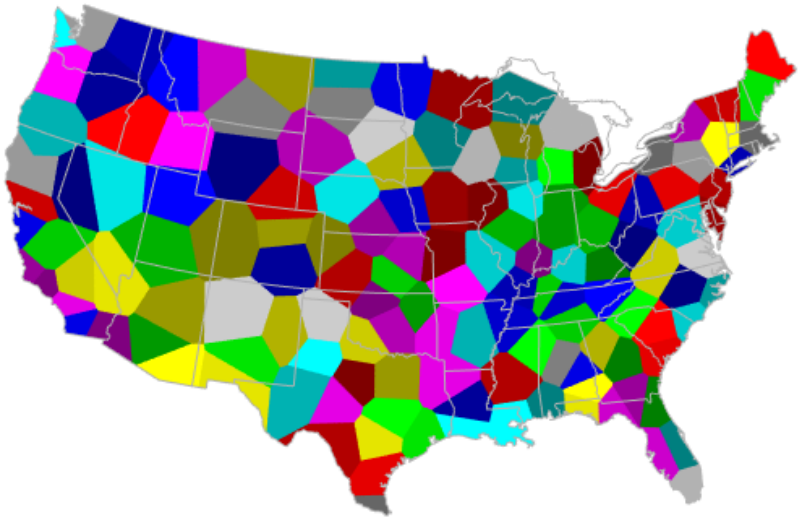

Figure 2-5. Area closest to each NEXRAD depicted in contrasting colors. Vertical weather occurrence histograms were aggregated within each area.

The TRACON-specific vertical weather histograms, normalized to sum to unity across all altitude bins, are shown in Figure 2-6. Of particular note is that some have very low altitude distributions of precipitating weather. These examples mainly occur on the West Coast, especially in the Pacific Northwest, which is consistent with the well-known scarcity of energetic convection in that region. Consequently, low altitude radar coverage would be of relatively greater importance in TRACONs of those regions.

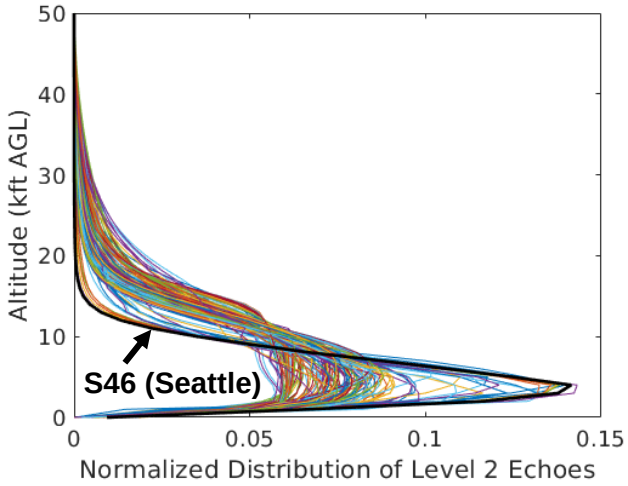

Figure 2-6. Computed vertical distributions of Level 2+ weather for each of the 146 TRACONs in this study.

2.1.1 Overall Results

We now present the computed coverage results. First, the percentage of area within each TRACON that exceeds a given WFVO threshold was computed for ASRs, WX radars, and ASRs + WX radars. Table 2-2 rolls up those results by giving the median computed over all TRACONs; the bottom row shows the percentage of TRACONs where the results for WX radars were better than for ASRs. The change in results with the minimum WFVO threshold, i.e., WX coverage faring better at lower thresholds, is indicative of the respective missions of the two radar types. Whereas ASRs are sited specifically to provide coverage near airports, NEXRADs and CANRADs are sited to provide more seamless coverage on a continental scale. Therefore, WX radar coverage is perfect everywhere if the vertical coverage requirement is more relaxed, while ASR coverage may be completely absent in far reaches of some of the larger TRACONs. If the vertical coverage requirement is stricter, then WX radar WFVO shows more deficiencies where the radars are farther away from the TRACONs.

We can also have a single 3D coverage value per TRACON by computing the mean WFVO inside the TRACON boundary; these are shown in the last column of Table 2-2. With this formulation, the overall coverage that would be provided by WX radars to TRACONs is quite close to the coverage provided by the ASRs alone, and 43% of TRACONs would have better coverage with WX radars. Of course, if WX radar coverage is added to the ASR coverage, then the combined coverage is greater than either alone.

Table 2-2

Median % of TRACON Area Exceeding WFVO Threshold

Radar Type	Minimum WFVO Threshold					3D Coverage (%)
	0.5	0.6	0.7	0.8	0.9	
ASR	99.7	99.6	99.3	98.7	92.7	96.4
WX	100	100	100	99.1	82.7	94.2
ASR + WX	100	100	100	100	99.6	98.4
% of TRACONs WX > ASR	67.1	66.4	59.6	50.0	42.5	44.4

We also computed the same metrics over near-airport airspace (range within 6 NM of the airport tower) of all associated towers (Table A-3) inside the TRACON boundary. This was done to focus attention on low-altitude coverage that may be operationally important for take-offs and landings. The overall median results are given Table 2-3. Somewhat counterintuitively, WX radars fare better than the ASRs in this space. We attribute this trend to the ASRs' cone of silence over their host airports, as well as the use of the high beam on receive at close range. The former cuts off high altitude coverage, while the latter overshoots low

altitude coverage, which together lowers WFVO at short ranges. The take-away message from Tables 2-2 and 2-3 is that WX radars alone would provide better coverage than ASRs in a significant fraction of TRACONs, especially for near-airport airspaces; and if they are added to ASRs, then we would have close to perfect 3D coverage on average.

Table 2-3

Median % of Airport Area (r < 6 NM) Exceeding WFVO Threshold

Radar Type	Minimum WFVO Threshold					3D Coverage (%)
	0.5	0.6	0.7	0.8	0.9	
ASR	95.3	93.4	90.6	86.7	69.1	90.5
WX	100	100	100	100	91.9	96.2
ASR + WX	100	100	100	100	100	99.0
% of TRACONs WX > ASR	65.1	63.7	61.6	57.5	53.4	66.2

The 3D coverage values per TRACON from which the overall medians of Tables 2-2 and 2-3 were computed are provided in Table B-1 of Appendix B.

2.1.2 Highest Benefit TRACONs for WX Radar Addition

We now present the TRACONs that would have the highest positive coverage difference if WX radars are added to ASRs. The top sites are given in Table 2-4. ASE (Aspen, CO) is the only TRACON in this study without any ASR coverage, so it would gain the most from WX radar coverage (Figure 2-7, left). Roughly a third of P50 (Phoenix, AZ), in the north, is entirely missing ASR coverage (Figure 2-8), and it comes in second. Note that P50 is the only TRACON that receives CARSR weather feed data to supplement coverage in the northern sector. Thus, on one hand, it might be argued that the benefit of having WX radar coverage is somewhat offset by the CARSR data. On the other hand, CARSR weather data quality (Carmouche 2012) and update period (108 s) are significantly worse than ASR weather data.

Table 2-4

3D Coverage (%) in Highest Benefit TRACONs for WX Radars

TRACON ID	ASR	ASR + WX	Difference
Aspen (ASE)	0	83.6	83.6
Phoenix (P50)	54.1	93.1	39.1
Boise (BOI): Bozeman (BZN) only	0	34.4	34.4
Missoula (MSO)	59.6	90.9	31.4
Las Vegas (L30)	61.4	87.3	25.9
Boise (BOI)	43.5	62.0	18.5
Salt Lake City (S56)	78.2	93.0	14.8
N. California (NCT): Reno (RNO) only	82.5	92.7	10.3
Roanoke (ROA)	86.1	95.3	9.2

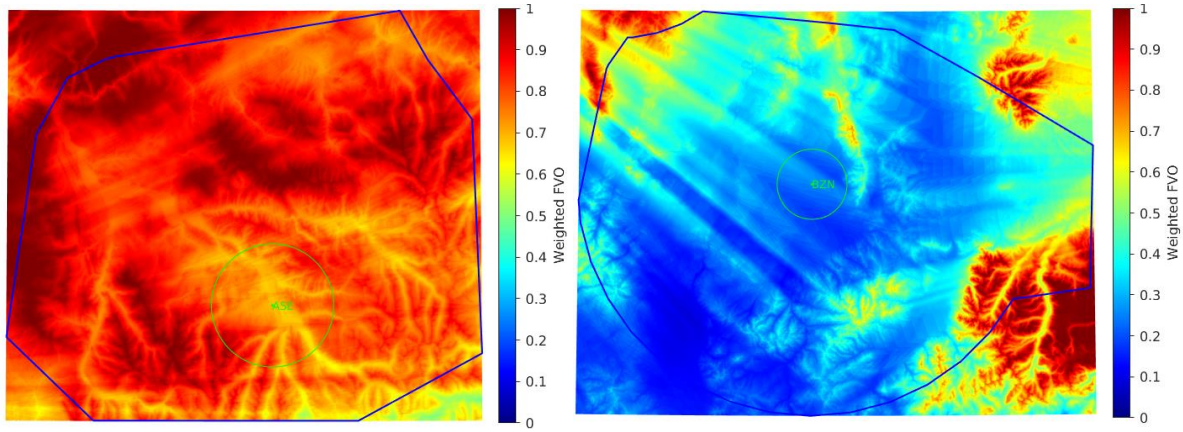

Figure 2-7. WX radar WFVO for Aspen (ASE) TRACON (left) and Bozeman (BZN) airspace (right). Both have zero ASR coverage. BZN is a secondary airspace of the Boise (BOI) TRACON.

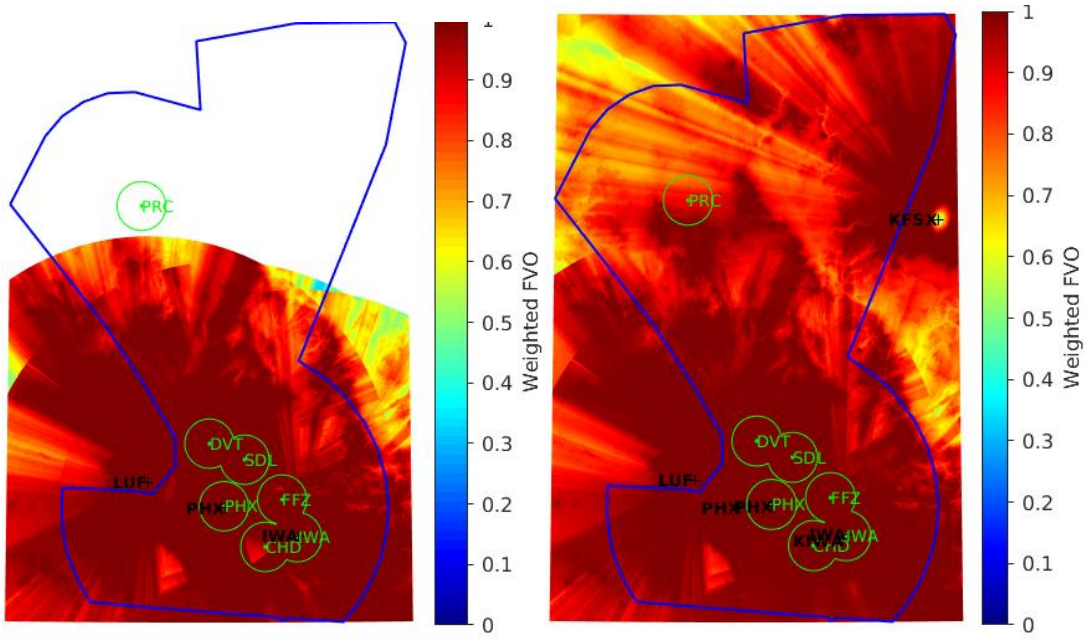

Figure 2-8. Phoenix (P50) TRACON WFVO for ASRs (left) and ASRs + WX radars (right). TRACON boundary is blue, radars labels are black, and 6-NM radii around airport towers are in light green. White space indicates lack of coverage.

BZN (Bozeman, MT) is a secondary airspace controlled by BOI (Boise, ID) and does not have its own ASR. However, unlike the ASE case, the WX radar coverage is poor, so even though there is a significant gain in coverage compared to 0, the resulting coverage is still not very good (Figure 2-7, right). When all of the airspace controlled by BOI is considered, i.e., BOI plus BZN, the gain in coverage with WX radars comes mainly from the added BZN coverage.

In MSO (Missoula, MT), the mountainous terrain blocks ASR coverage at the farther reaches of the TRACON airspace. Adding WX radar coverage coming from a nearby NEXRAD, sited at a higher altitude, fills in these gaps (Figure 2-9).

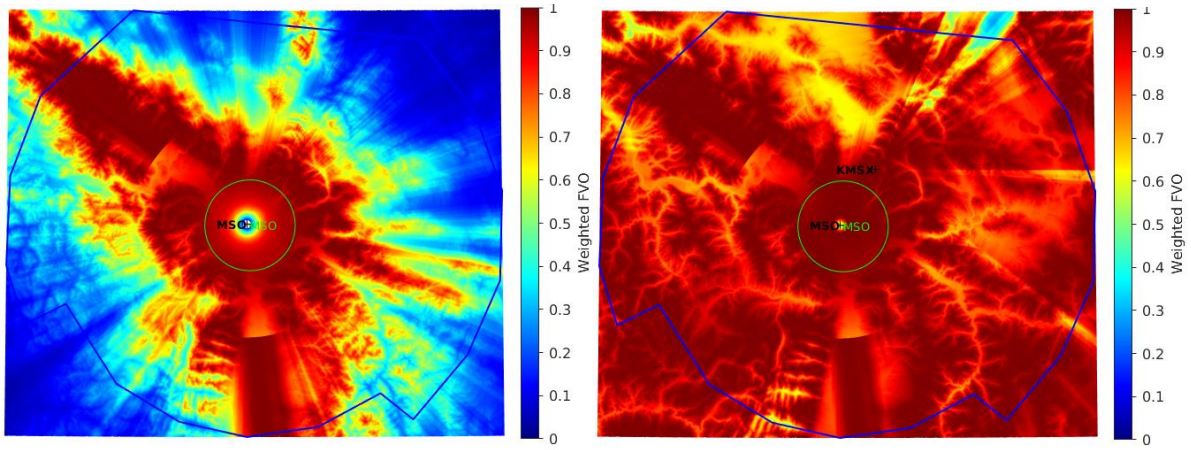

Figure 2-9. Missoula (MSO) TRACON WFVO for ASRs (left) and ASRs + WX radars (right).

In the L30 (Las Vegas, NV) TRACON, some deficiency in coverage in the eastern sector that would be left by the removal of the LAS ASR as part of the divestiture plan, would be nicely filled in by WX radar coverage (Figure 2-10). In comparing the ASR coverage for current vs. post-divestiture states, we found that of the 34 TRACONs affected by the ASR divestiture program, 33 of them would experience less than 5% difference in mean WFVO coverage. The exception, L30, would go from 79.5% (now) to 61.4% (post-divestiture), for an 18.1% decrease. We recommend considering removing the LSV ASR instead of the LAS ASR, which, we compute, would lead to only a decrease of 5.7% in WFVO.

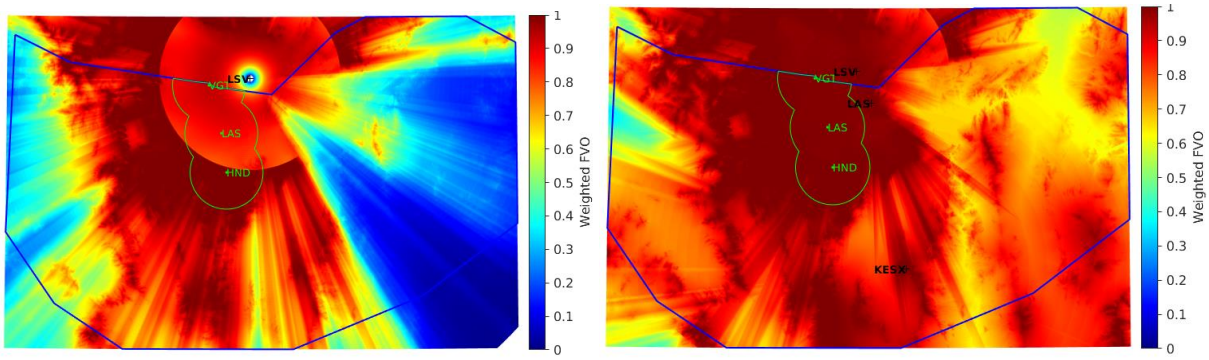

Figure 2-10. Las Vegas (L30) TRACON WFVO for ASRs (left) and ASRs + WX radars (right). The addition of WX radars fills in the areas of poor coverage (blue colors) in the left-hand plot.

It is noteworthy that the top benefit sites for WX radars are in the mountainous western U.S. (The first non-western site that appears on this list is ROA (Roanoke, VA), which is in the heart of the Appalachian Mountains.) Terrain blockage plays a significant role in limiting the range of ASRs in these locales, as they are sited on relatively low ground (i.e., valleys) where airports are located. The Salt Lake City (S56) TRACON is a good example of this (Figure 2-11). Because NEXRADs are deployed for overlapping long-range coverage, they tend to provide wider coverage within TRACONs, and would certainly be excellent complements to ASRs in these TRACONs, helping to address shortfall #4 (coverage) for the STARS precipitation display.

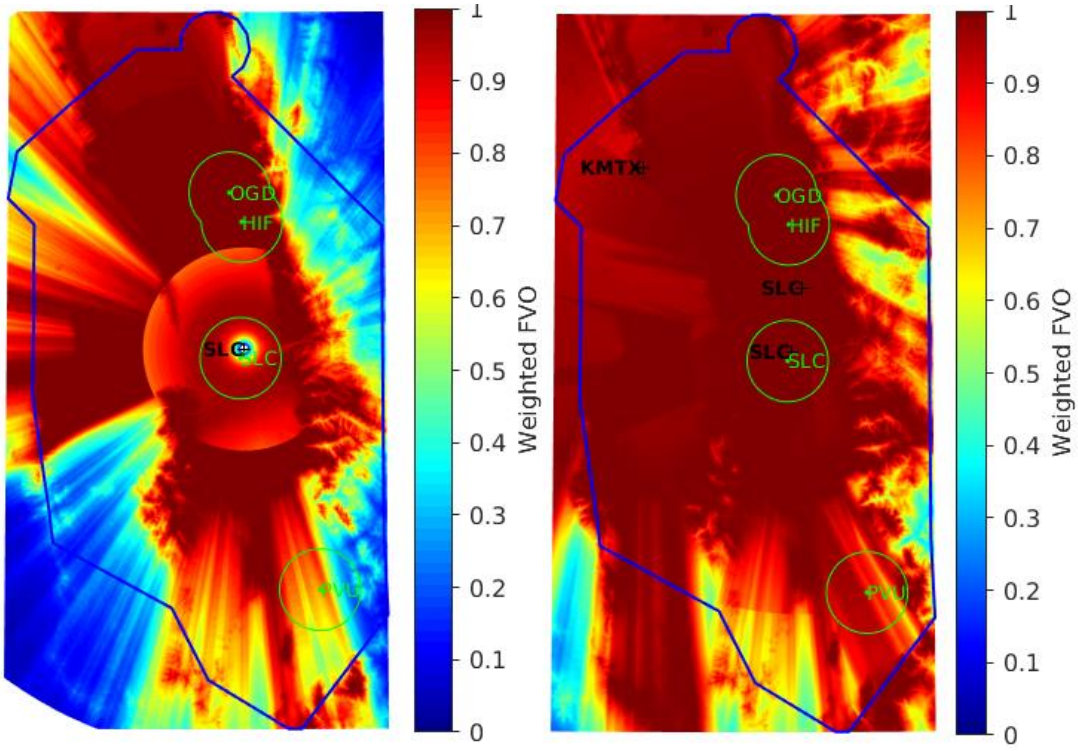

Figure 2-11. Salt Lake City (S56) TRACON WFVO for ASRs (left) and ASRs + WX radars (right). The SLC ASR, located at airport level, is blocked by surrounding mountains in multiple directions (areas of blue in left plot). The higher elevation NEXRADs, especially KMTX, help fill in those gaps (right plot).

2.1.3 TRACONs with Worst Coverage by WX Radars

We now turn our attention to the other end of the coverage spectrum—the TRACONs with the biggest losses when comparing ASR to WX radar coverage (Table 2-5). This list is important if, in the future, there is consideration for eliminating ASR weather data requirements in favor of having a terminal precipitation display product being entirely generated from weather radar data.

Table 2-5

3D Coverage (%) in TRACONs with Worst Coverage by WX Radars

TRACON ID	ASR	WX	Difference
Eugene (EUG) w/o Medford (MFR)	90.5	38.1	-52.4
Moses Lake (MWH)	94.5	57.2	-37.3
Eugene (EUG)	88.8	55.8	-33.0
Roswell (ROW)	97.6	66.9	-30.7
Casper (CPR)	93.3	64.6	-28.7
Bangor (BGR)	93.8	71.4	-22.4
Reading (RDG)	97.9	79.9	-18.0
Harrisburg (MDT)	96.7	79.8	-16.9

Because the Eugene, OR (EUG) TRACON has responsibility over Medford, OR (MFR) airspace, which is physically separated, we computed the coverages over each area separately. The first entry in Table 2-5 is EUG without MFR, and the third entry is EUG and MFR combined. (The MFR-only case did not make this list.) Figure 2-12 shows that the worst coverage from the WX radars occurs right in the middle of the EUG TRACON. This is due to this area being about the farthest point between the Portland, OR NEXRAD (KRTX) and the Medford NEXRAD (KMAX). The combination of the lack of near-surface coverage and the prevalence of low-altitude weather in the Pacific Northwest (Figure 2-6) makes west-central Oregon most problematic for WX radar coverage. This can also be seen in daily maximum composite reflectivity data (Figure 2-13).

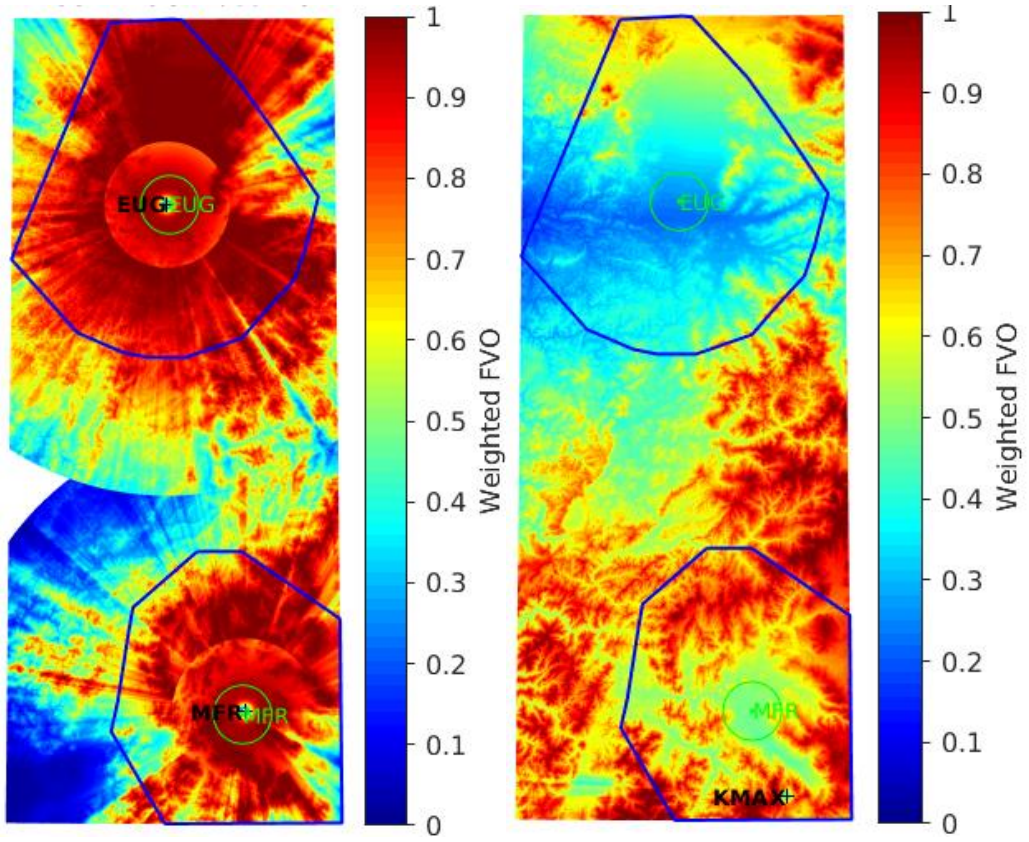

Figure 2-12. Eugene (EUG) TRACON and Medford (MFR) airspace WFVO for ASRs (left) and WX radars (right).

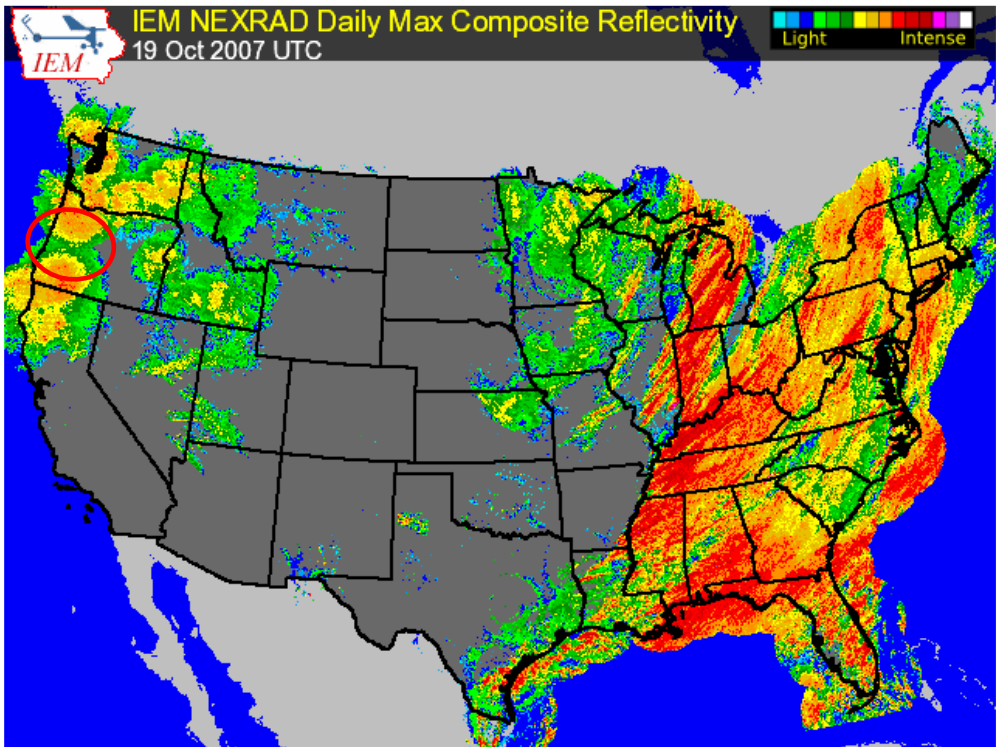

Figure 2-13. NEXRAD daily maximum composite reflectivity example. From the Iowa Environmental Mesonet (IEM) web site (https://mesonet.agron.iastate.edu/docs/nexrad_mosaic/). Coverage seam in west-central Oregon is highlighted by red oval. KMAX's lowest elevation angle has since been lowered from 0.5° to -0.1°, which helps but does not eliminate the coverage deficiency.

WX radar coverage over the Moses Lake, WA (MWH) TRACON is sparse in the western sector (Figure 2-14), due to the far distance of the Seattle, WA NEXRAD (KATX) and its blockage by the high Cascade mountain range. CANRADs also contribute little due to distance and mountain blockage. The southern half of the Roswell, NM (ROW) TRACON also suffers from radar distance and terrain obscuration (Figure 2-15).

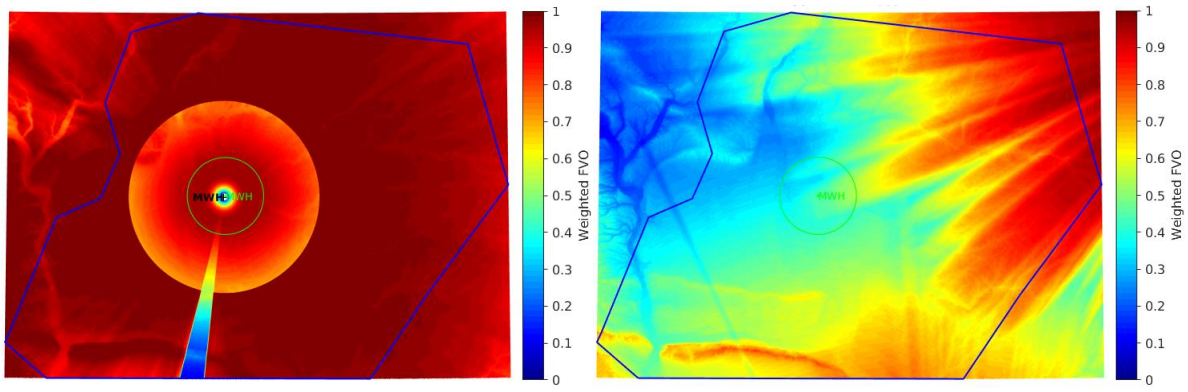

Figure 2-14. Moses Lake (MWH) TRACON WFVO for ASRs (left) and WX radars (right).

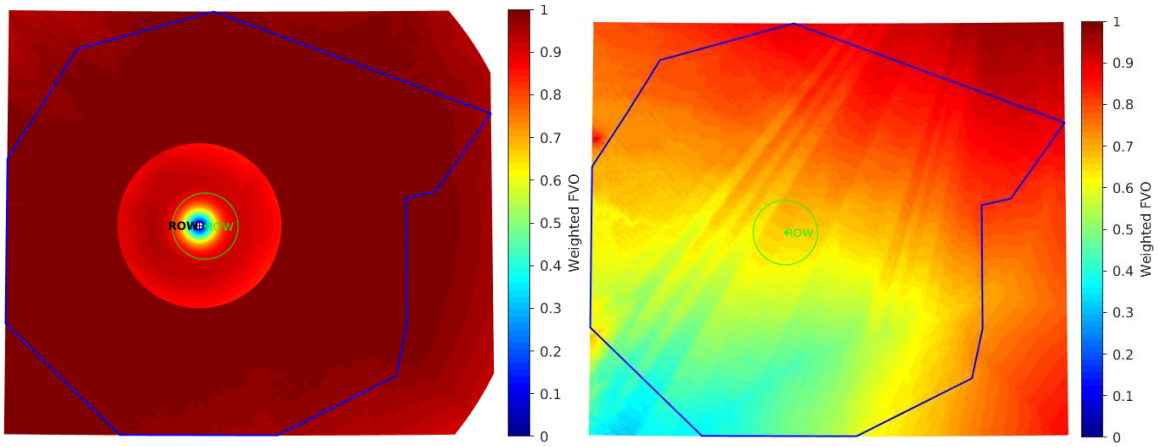

Figure 2-15. Roswell (ROW) TRACON WFVO for ASRs (left) and WX radars (right).

Further down the list are TRACONs in the eastern U.S. Here, terrain blockage is a less significant issue than in the West—it is more a case of WX radars not being located very close to the TRACONs. For these cases, the WX radar coverage often appears fairly smooth and consistent (e.g., Figure 2-16), albeit with WFVO not as high as for the ASRs. This begs the question of what coverage level would be deemed acceptable for ATC operations. Figure 2-17 shows histograms of 3D coverage per TRACON. There is a fair amount of variance in the 3D coverage provided by ASRs, especially for the near-airport case (Figure 2-17, top right), but most cases fall into bins above 80%, which suggests that perhaps 80% 3D coverage may be acceptable in most cases. However, is "acceptable" 3D coverage dependent on other factors such as traffic volume and frequency of hazardous weather? As there is no pre-existing FAA requirement along

these lines, we recommend further evaluation through human-in-the-loop exercises comparing ASR-based and WX-radar-based precipitation products side by side. The benefit of adding WX radar coverage to ASR coverage is clearly shown in the bottom two histograms in Figure 2-17, as the combined 3D coverage is nearly all greater than 90% for both TRACON and near-airport airspaces.

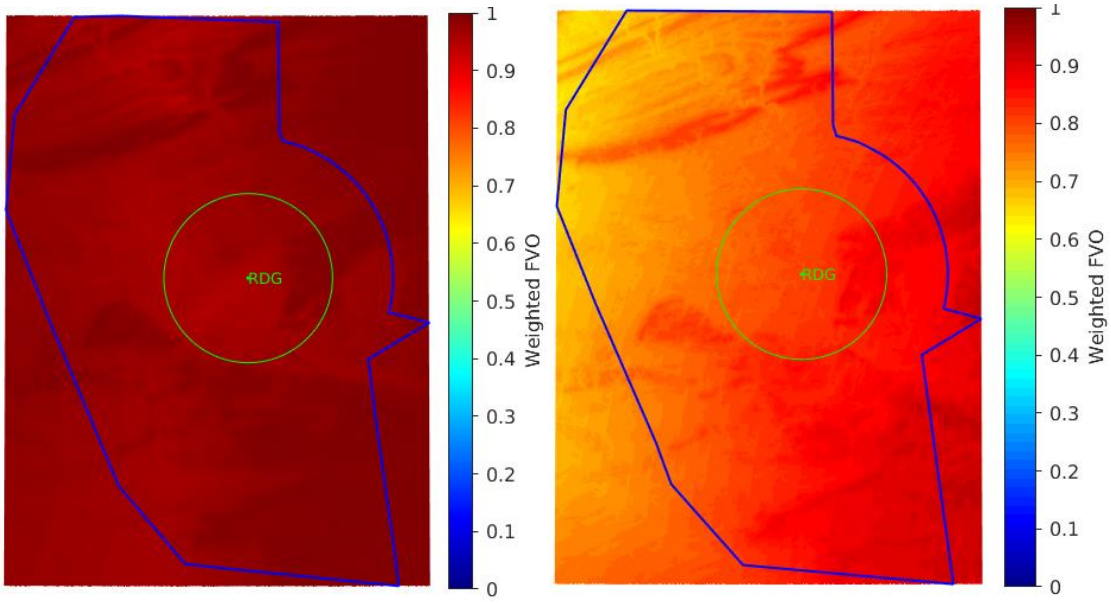

Figure 2-16. Reading (RDG) TRACON WFVO for ASRs (left) and WX radars (right).

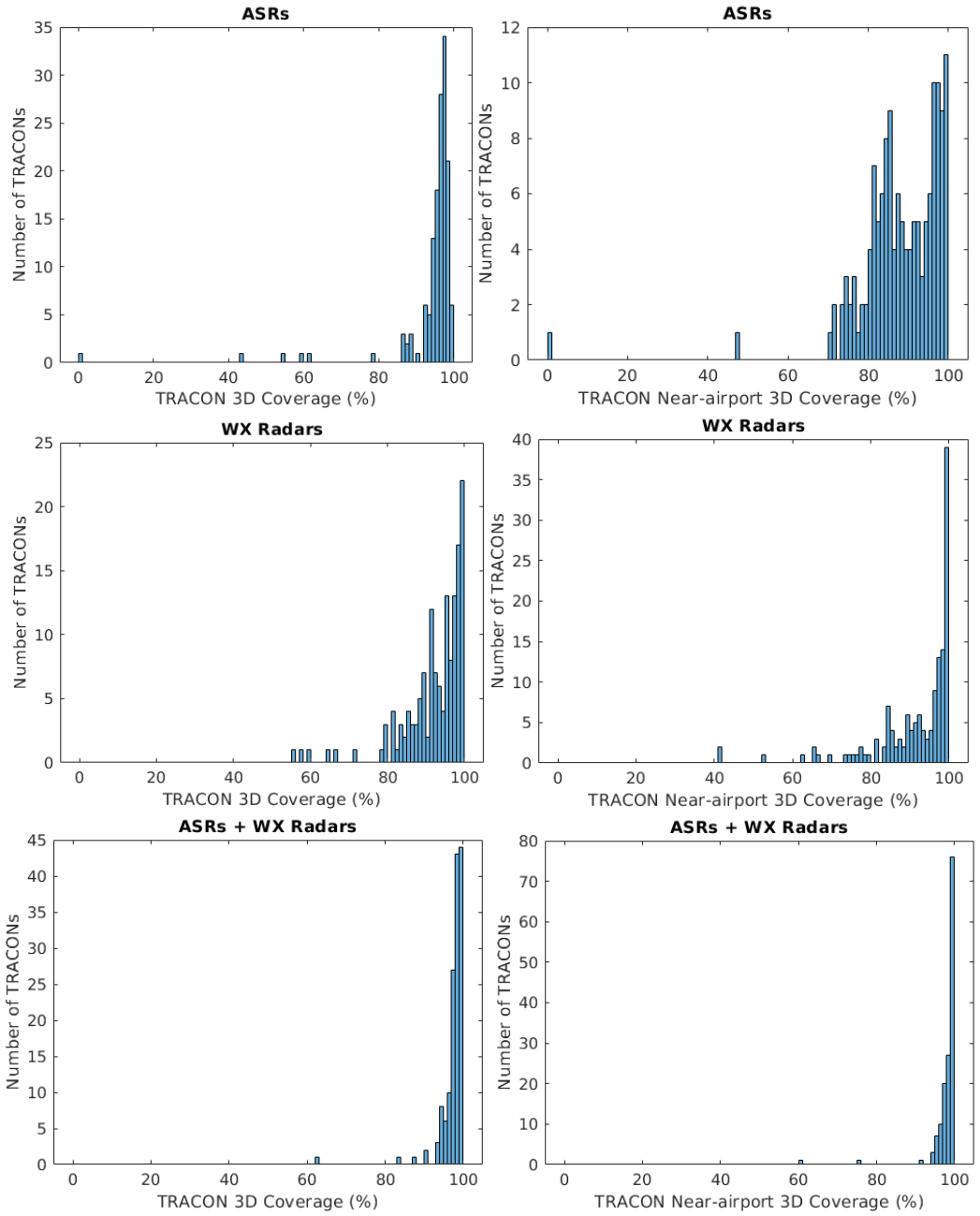

Figure 2-17. Histograms of 3D coverage for ASRs (top row), WX radars (middle row), and ASRs + WX radars (bottom row).

If we assume for the moment that 80% 3D coverage is the minimum acceptable threshold, then we can narrow the list of the top coverage benefit sites (for the addition of WX radars to ASRs, as given in Table 2-4) to ones where the ASR coverage is less than 80%. The resulting list is ASE, P50, BOI, MSO, L30, and S56. Analogously, we can narrow the list of potentially problematic sites (for WX radars alone, as given in Table 2-5) to ones where the WX radar coverage is less than 80%. Rounding to the nearest integer, we have EUG, MWH, ROW, CPR, and BGR.

2.2 HORIZONTAL RESOLUTION

The horizontal resolution of the 2D precipitation products displayed on STARS is dependent on many factors. Because there are numerous processing steps between data acquisition by the radar and display of the final product on the controller's "glass," the effective resolution is limited not only by the radar pulse resolution volume, but by the various averaging that is necessitated by data quality needs. Furthermore, these factors are independent of the quantized output intervals of the intermediate and final data.

Briefly, the azimuthal resolution of radar data is limited by: 1) antenna beam width (BW), 2) coherent processing interval (CPI), 3) azimuthal smoothing, and 4) data output interval. Radar data range resolution is limited by: 1) transmitted pulse width and processing, 2) range smoothing, and 3) data output interval. For more details on these issues, see Doviak and Zrnic (1993).

After the radar data is ingested by the NextGen Weather System, further processing (resampling to Cartesian coordinates, etc.) alters the end-product horizontal resolution. Here, we wish to investigate whether the native horizontal resolution of weather radars presents any concerns or potential benefits relative to the effective horizontal resolution being provided by ASRs for the STARS precipitation display.

Table 2-6 gives the azimuthal and range resolutions for reflectivity data from the WX radars and the 6-level VIP product from the ASRs. The range resolution given is, strictly speaking, slant range resolution, which differs slightly from ground range resolution. However, for our purposes and the relatively low elevation angles of interest, they can be taken to be the same. The procedure for computing the effective azimuthal resolution from the antenna BW and CPI is explained in section 7.8 of Doviak and Zrnic (1993). NEXRAD's so-called "super resolution" technique employs tapered windowing of time series data and a 0.5° output interval to achieve an effective resolution of 1° (Torres and Curtis 2007). ASR-9 6-level weather product generation and associated data averaging is discussed in FAA (2008). The ASR-11 averaging is dependent on the weather intensity levels, and is site-adjustable, so the 3 x 3 (azimuth x range) averaging assumed here is the worst-case scenario (Regulus 2020). The upgraded ASR-8 appears not to perform any spatial smoothing on the precipitation product (IE 2019).

Table 2-6

Radar Spatial Resolution Parameters

Radar	Azimuth					Range (km)			
	BW	CPI	Output Interval	Averaging	Effective	Pulse	Output Interval	Averaging	Effective
NEXRAD	0.95°	1°	0.5°	N/A	1°	0.25	0.25	N/A	0.25
TDWR	0.55°	1°	1°	N/A	1.2°	0.15	0.15	N/A	0.15
CANRAD	0.9°	1°	1°	N/A	1.5°	0.5	0.5	N/A	0.5
ASR-8	1.4°	1.4°	1.4°	N/A	2°	0.15	0.93	N/A	0.93
ASR-9	1.4°	1.4°	1.4°	3 x	4.8°	0.15	0.93	3 x	2.8
ASR-11	1.4°	1.4°	1.4°	3 x	4.8°	0.15*	0.93	3 x	2.8

*After pulse compression processing.

We can see from Table 2-6 that the WX radar reflectivity outputs provide superior horizontal resolution relative to the ASRs. Some of this advantage in the azimuth dimension may be counteracted if the WX radars are located farther away from the TRACON than the ASRs. To investigate this issue, we computed the limiting horizontal resolution (LHR), which is the worse of either the azimuthal or range resolution at any given point in space, over all the TRACONs. The mean LHR computed over each TRACON and over the near-airport airspaces are listed in Table B-2 of Appendix B. The median of these values computed over all the TRACONs are given in Table 2-7.

Table 2-7

Median LHR (km) Over All TRACONs

Domain	ASR	WX	ASR+WX	% of TRACONs WX < ASR
TRACON	4.02	1.18	1.14	93.4
Within 6 NM of Airports	2.79	0.89	0.87	88.4

The LHR statistics show that the horizontal resolution of WX radar data that are ingested by the NextGen Weather System is better on average than that of the ASR six-level precipitation product that is sent to STARS. Of the small number (11) of TRACONs where WX LHR is worse than ASR LHR, only Casper, WY (CPR) has a mean TRACON LHR that is more than 1 km greater for WX radars. Thus, we might reasonably expect a benefit associated with this resolution improvement, for both WX radar data as supplement to ASR data and even for WX radar data alone. Since better spatial resolution contributes to a more accurate depiction of weather, this will help address shortfall #1 (accuracy) for the STARS

precipitation display. The actual horizontal resolution of the WX-radar-based STARS precipitation display will be limited by the 1-km grid spacing of the NextGen Weather System and potentially by TPoG adaptor processing. Ideally, the NextGen Weather System Cartesian grid would be directly ingested and displayed by STARS, but the current STARS input only accepts radar-based range-azimuth grids, so the NextGen Weather System data will need to be resampled as virtual radar data input, which will degrade the horizontal resolution at points farther away from the virtual radar locations. In addition, the STARS reprojection and mosaicking algorithm further modifies the virtual radar resolutions prior to display on the scope.

Note, however, that finer horizontal resolution may not necessarily be better from an operational perspective. Even if accurate, there may be instances when fine-scale differences in precipitation levels might distract more than help in routing traffic. There is likely an optimal resolution for TRACON operations. But it certainly is better that the input radar data have finer than coarser resolution, because it is possible to further smooth the former but impossible to recover finer features from coarser data.

3. TIME DOMAIN ANALYSES

We now shift to a discussion of time domain issues that are relevant for the TPoG program. As shortfall #5 for STARS precipitation display is insufficient availability of event depiction, the input radar data availability is certainly a matter of interest. Timely depiction of precipitation on the STARS display is also an important factor, which involves both update period and latency of the input data. We begin with an analysis of data availability.

3.1 OPERATIONAL AVAILABILITY

The availability of STARS precipitation display data is a product of the individual availabilities of all components, starting with the radars, through the various processors, and the data transfer lines. Of all the components, radars are the most likely culprit to be the limiting factor in the end-to-end operational availability (A_o) chain. This is because radars require a significant amount of scheduled maintenance downtime every year. Operational availability includes scheduled downtime, in contrast to inherent availability (A_i), the metric most often used for specification in contracts. As the name suggests, operational availability is more relevant for practical operational concerns.

The A_o specification for the ASRs (FAA 2017) and TDWR is 0.999 (FAA 1987). For NEXRAD, it is 0.960 for the National Weather Service (NWS) and Air Force (AF) systems, and 0.989 for the FAA systems (ROC 2008).

If there is overlap of coverage from different radars, then the aggregate data availability in that area of overlap will be greater than the individual radar data availability. Therefore, adding a WX-radar-based precipitation product to the existing ASR-based STARS display will increase the overall availability of the displayed data. The formula for this aggregate operational availability is

$$A_o(N) = 1 - [1 - A_o(1)]^N , \quad (1)$$

where N is the overlap count. Using the actual recent A_o statistics for each radar type (not shown here), the formula revealed that all of them would exceed 0.999 A_o with two overlaps, except for the FAA NEXRAD. (The only FAA NEXRADs relevant for this study are the ones in Alaska, where hazardous convective weather is rare.)

Figure 3-1 shows histograms of the average coverage overlap counts per TRACON; the left column shows results for averaging over the TRACON area, and the right column shows results for averaging only over near-airport areas. Individual TRACON results are given in Appendix B, Table B-3. For the TRACON-averaged cases, only 32 out of 146 TRACONs (22%) have average ASR coverage overlap of two or more, while 131 out of 146 TRACONs (90%) have average WX radar overlap of two or more. This implies that the WX radars tend to have much better aggregate TRACON A_o than the ASRs. And when the two sources are combined, no TRACON would have single-radar coverage, meaning that the TRACONs

would have $A_o > 0.999$ even with the historical single-radar A_os. Therefore, a WX-radar-based precipitation product on STARS would help address shortfall #4 (availability) for the STARS display. The near-airport cases show similar benefits.

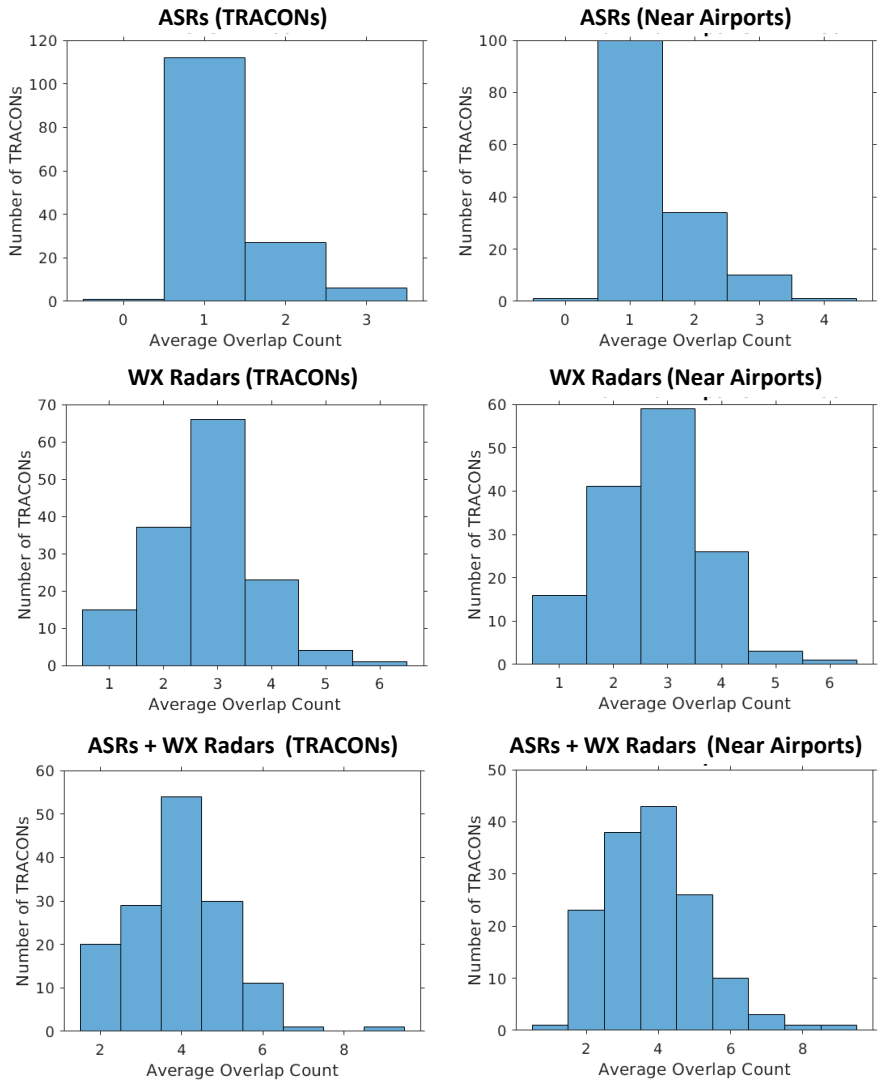

Figure 3-1. Histograms of average coverage overlap count in a TRACON for ASRs (top row), WX radars (middle row), and ASRs + WX radars (bottom row). The left column is average taken over the TRACON, and the right column is average taken over near-airport (r < 6 NM) airspace.

3.2 UPDATE PERIOD

The timeliness of the STARS precipitation display depends on the update period—which is the time elapsed between display updates—and latency—which is the time elapsed between the start of radar observation to display presentation. The update period for the ASR-based STARS weather display is 28.8 s, and it would be 25 s for a NextGen Weather System-based STARS weather display. Therefore, the two update periods are comparable, and there would not seem to be any concerns in this area. However, these update periods only correspond to the output of the data processors—they do not necessarily mean that the inputs to the processors are being refreshed with new observations at the same or faster rate. If they are not, then the timeliness of the display can be worse than the stated update period.

The ASRs perform a 360° azimuthal rotation of its vertically thick (Figure 2-2) antenna beam every 4.8 s, average the weather reflectivities over six scans, then output the temporally smoothed six-level precipitation product to STARS. Thus, its 28.8-s update period is reflective of the actual observational refresh time. The situation is not as clear for the NextGen Weather System, because it ingests data from multiple WX radars with variable scan update periods. Also, unlike the ASRs, the WX radars conduct 360° azimuthal rotations of vertically thin (Table 2-1) antenna beams at multiple elevation angles to cover the surveillance volume. Thus, it would be useful to understand, at least on average, how often new and independent WX radar observations are going into each 25-s NextGen Weather System update. For this investigation, we focus on the NEXRAD for specific details, since it is the dominant source of radar data for the NextGen Weather System.

First, we note that NEXRADs have, since 2012, a scanning mode called automated volume scan evaluation and termination (AVSET; Chrisman 2013), which is turned on by default at all sites. AVSET determines the highest elevation angle where there are detectable weather echoes and skips the scanning of higher angles (Figure 3-2) with some added margin for rapid growth. The result is that nearly every elevation scan has new weather observation data, i.e., there is little “wasted” radar time spent on clear-air elevation cuts. This implies that almost every new elevation scan received from a NEXRAD by the NextGen Weather System contains fresh precipitation data. AVSET also reduces the average volume scan update periods. For example, the median volume update time for NEXRAD VCP 12, a popular severe weather VCP, is 3.6 minutes. The median NEXRAD volume update time for all non-clear-air VCPs is 4.6 minutes. (TDWRs have even faster volume scan updates for hazardous modes at about 2.5 minutes.)

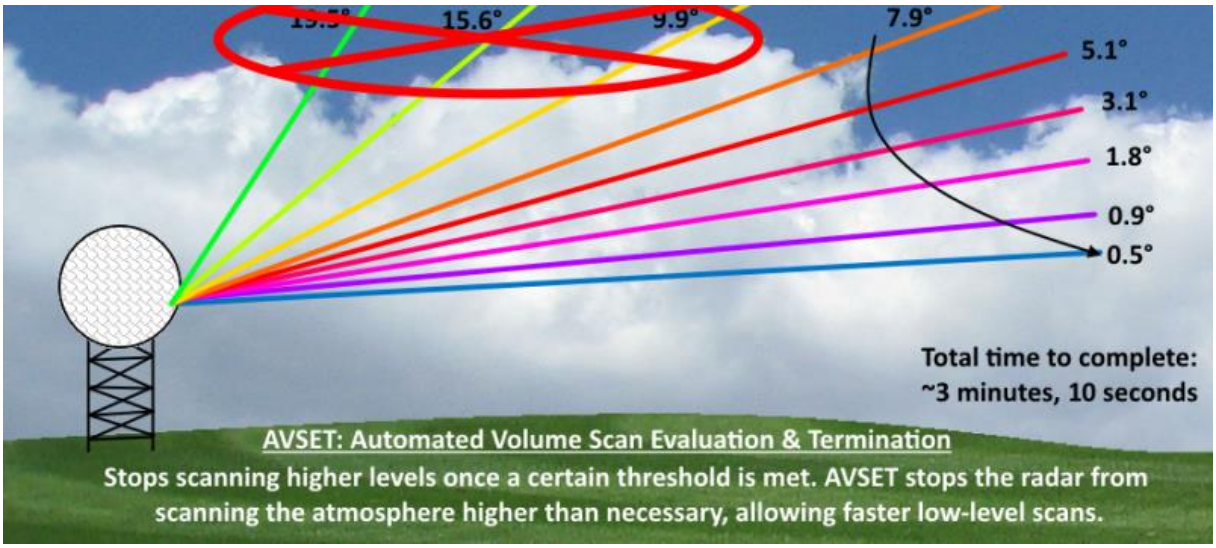

Figure 3-2. Illustration of AVSET. From Mersereau (2014).

Second, as with availability, overlapping coverage provides a boost to update rates. For radars scanning 360° azimuthally every T seconds, at any given point in 3D space, the mean revisit period by a radar is T/N, where N is the overlap count. However, at a given point in horizontal space, N varies with altitude due to the Earth's curvature, ground blockage, and radar cones of silence (Figure 3-3). Furthermore, every altitude is not of equal importance, since the occurrence of weather varies with height at each location. Therefore, for every point in 2D horizontal space, we calculated the weighted mean update time using the product of the overlap count and Level 2 reflectivity (Figure 2-6) vertical profiles. We assumed T = 21.4 s, which is the actual average elevation scan time, taken over 2014-2020 for all CONUS NEXRADs in non-clear-air VCP modes. (The average TDWR elevation scan update period is about 15 s.)

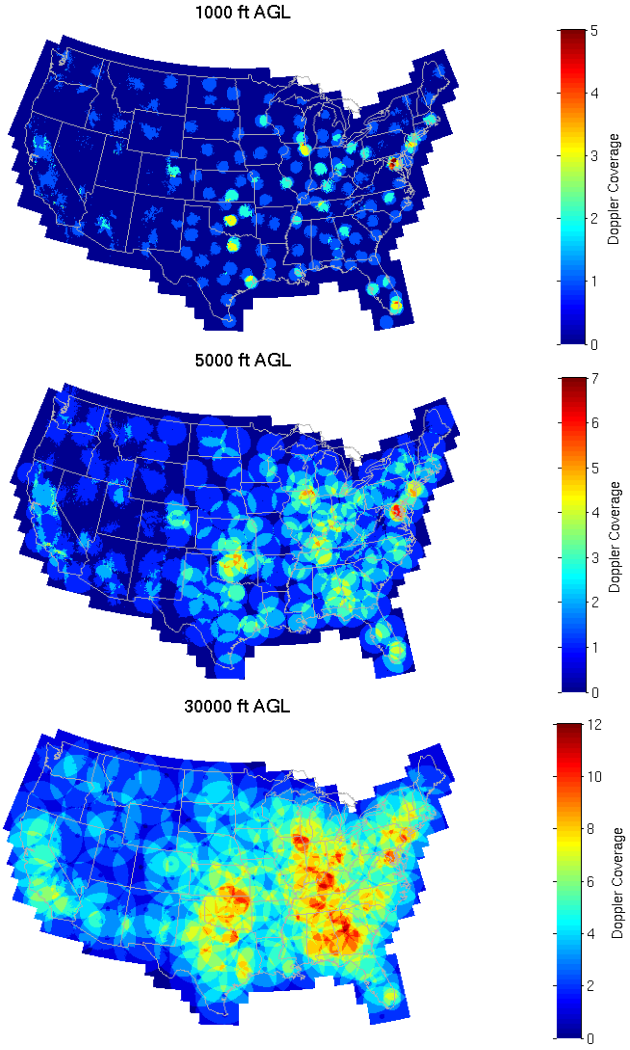

Figure 3-3. NEXRAD and TDWR coverage overlap count by altitude. From Cho (2015).

The resulting weighted mean WX radar update times averaged over each TRACON and over the near-airport areas are given in Appendix B, Table B-4. The histogram of the TRACON results is shown in Figure 3-4. Two extreme cases are plotted in Figure 3-5—Chicago, IL (C90) and Anchorage, AK (A11). C90, due to the high number of radar coverage overlaps, has the shortest average WX radar update period (3.9 s), while A11, with coverage mainly from one NEXRAD, has an average update period of 21.3 s. The bulk of TRACONs would have a new and independent elevation scan every 5 to 10 s in the presence of weather, with a median value of 7.6 s—comparable to the ASR scan period of 4.8 s. (The median elevation scan update period of 7.6 s corresponds to a median overlap count of 2.8.) This is a conservative estimate,

since we used the average NEXRAD *T* as input, whereas TDWRs, as noted earlier, have shorter elevation scan periods. In general, TRACONs with longer effective WX radar update periods tend to be in locations with lower terminal traffic and convective weather hazard occurrence. (TRACONs with high traffic and convective hazard occurrence have TDWRs, which overlap with NEXRAD coverage.) We conclude that the NextGen Weather System receives fresh WX radar rapidly enough on average for its 25-s update period to be a meaningful measure of data timeliness.

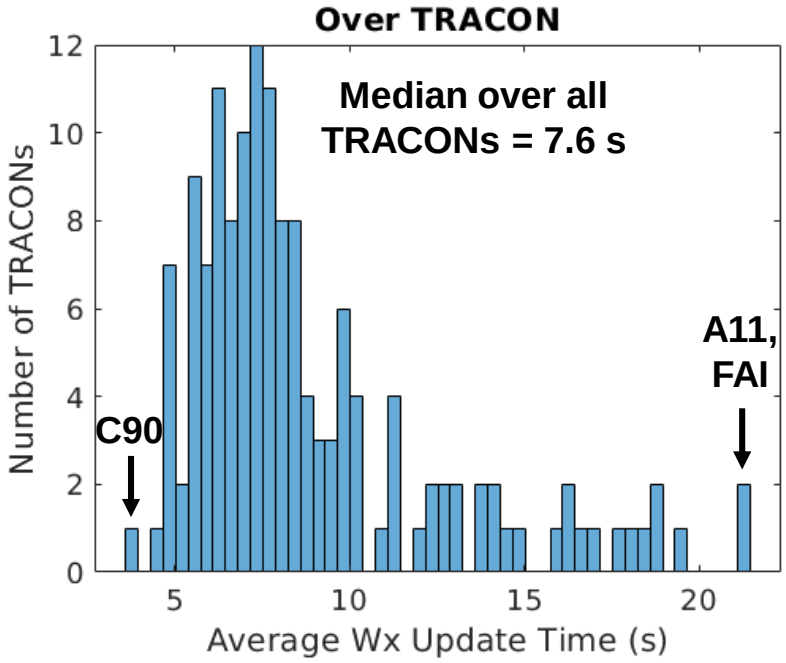

Figure 3-4. Histogram of weighted mean WX radar scan update times averaged over each TRACON.

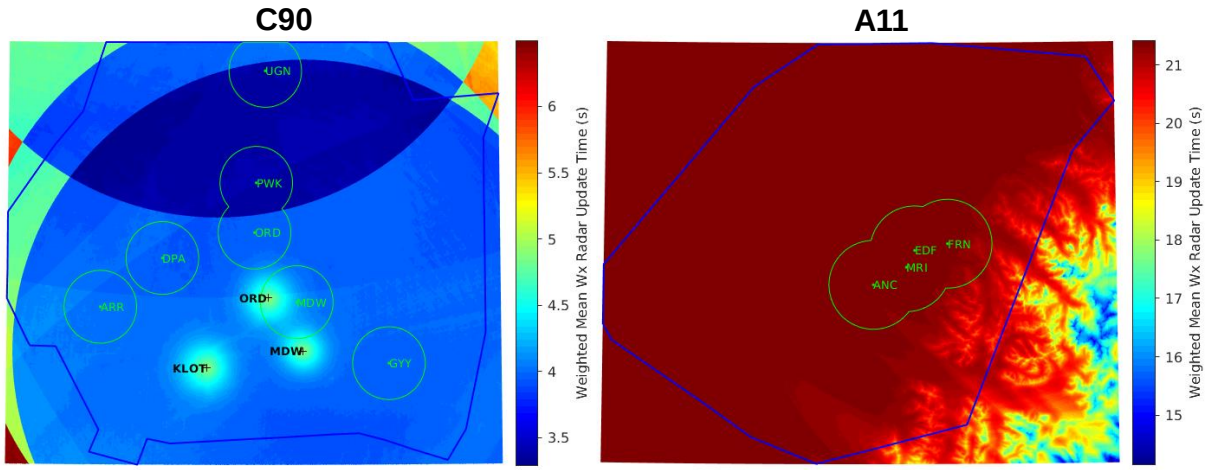

Figure 3-5. Weighted mean WX radar update period for the Chicago (left) and Anchorage (right) TRACONs. Note that the color scales for the two plots differ.

Although we have shown that there is meaningful data refresh within the 25-s update window of the NextGen Weather System, complete volume updates take a longer time. For any vertical column, the aggregate multi-radar volume update period depends on many factors. It would certainly decrease with the number of overlaps within a given vertical column. At best, it could be the single-radar volume update time divided by the degree of overlap if the radars happen to scan different elevations at different times, but at worst it could approach the single-radar update time if the radars happen to scan the same elevations at the same times. If we crudely assume that the distribution of cases is uniform between the two extremes, then we get $(T_v/N + T_v)/2$ for the average multi-radar volume update time, where T_v is the average single-radar volume update time. Applying this expression to the median NEXRAD non-clear-air volume update time of 4.6 minutes and the average overlap count of 2.8 over all TRACONs, we get 3.1 minutes as a very rough estimate of the average WX volume update period overall all TRACONs. This is likely an overestimate as it does not get credit for the faster volume update time (2.5 minutes) of TDWRs.

Unlike discrete targets like aircraft, precipitation has significant vertical continuity. Therefore, the horizontal location updates of precipitation that are generated faster than the full volume updates can be quite accurate, especially with the sliding volume time alignment scheme (discussed further in the next section) used by the NextGen Weather System. However, intensity measures like VIL and composite reflectivity that are computed over the vertical column are more accurate at the full volume update timescale. It would be prudent to conduct further comparative evaluation using real and/or simulated radar data to assess the overall suitability of a WX-radar-based precipitation product for airport and TRACON ATC operations.

3.3 LATENCY

No matter how often the display data is updated, if there is a long time lag between observation and display, then it cannot be said that the display is timely. This lag, or latency, between the start of radar observation and delivery of the processed six-level VIP data to the STARS display input is specified to be within nine ASR scans (Raytheon 1999), which is 9 × 4.8 s = 43.2 s. This latency definition excludes any reprojection and mosaic time by the STARS display processor. We now proceed to estimate the equivalent latency for a NextGen Weather System-based TPoG display on STARS.

For this analysis, we begin with the start of a NEXRAD scan and end with delivery of the TPoG six-level weather product at the STARS display input. Table 3-1 lists the component breakdown of the entire latency chain.

Table 3-1

Latency Budget for NextGen Weather System-based STARS Precipitation Data

Process	Latency (s)
Average NEXRAD elevation scan	21
NEXRAD Product 193 generation	5
NEXRAD to CSS-Wx data transfer	15
CSS-Wx provider service adaptor	1
NextGen Weather System data ingest and pre-processing	5
Average NextGen Weather System mosaic queue wait time	12.5
Mosaic trigger to Composite Reflectivity mosaic in netCDF	4
NextGen Weather System/CSS-Wx to cloud data transfer	5
Virtual radar data generation	5
Cloud to STARS data transfer	33 (T1), 10 (T2), 3 (T3)
STARS TPoG adaptor	10
Total	*116.5 (T1), 93.5 (T2), 86.5 (T3)*
Total with NextGen Weather System motion compensation	**53 (T1), 30 (T2), 23 (T3)**

As stated previously, 21 s is the average measured NEXRAD elevation scan time for non-clear-air VCPs. Product 193 is NEXRAD Level 3 super-resolution digital reflectivity with data quality algorithm processing that the NextGen Weather System ingests to generate CR or VIL (Dupree and Cho 2021) that will be used to produce the six-level precipitation product for STARS. Five seconds is a typically observed generation time for Product 193. The data would then be sent to the FAA's CSS-Wx system, with a data transmission and CSS-Wx provider service adaptor processing latency specifications of 15 s and 1 s, respectively (FAA 2021).

The average measured time for per-radar Product 193 ingest and pre-processing by the NextGen Weather System up to the multi-radar mosaic queue is 5 s. At this point, the data waits in the queue until the next mosaic trigger, which cycles every 25 s—therefore, we estimate the mean wait time to be 25/2 = 12.5 s, since individual radar scans can arrive at any point within the 25-s window. After the trigger, the measured average time for mosaic generation and conversion to netCDF format is 4 s (Greg Viola, private communication).

After this point, the future operational TPoG processing and dissemination architecture has not been determined. Thus, we assumed a particular architecture as illustrated in Figure 3-6. The NextGen Weather System output data is assumed to be sent via T3 transmission line to a virtual radar (VR) generation processor ("slicer") in a cloud computing environment. Based on 29 MB of NextGen Weather System output sliced data, we estimate about 5 s for this data transfer latency. Since some of the larger 146 TRACONs will require more than one VR for complete coverage, we assumed 300 VRs; for this cloud-based VR generation time, we conservatively allocated 5 s.

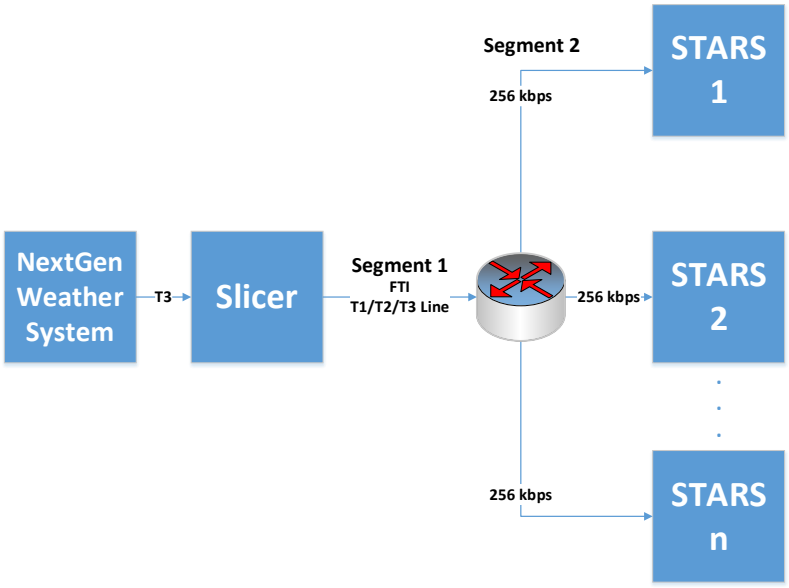

Figure 3-6. Assumed TPoG data distribution architecture.

The cloud-to-STARS transfer times given in Table 3-1 assumes T1, T2, or T3 transmission lines for Segment 1, and 256-kbps lines for Segment 2 (Figure 3-6). The 256 kbps bandwidth is based on an assumption that some facilities may be still using older equipment. Finally, the STARS TPoG adaptor processing time of 10 s is conservatively based on current concept demonstration system performance. The

resulting total latency times are about a factor of two longer than the 43.2-s specification for the ASR six-level weather product delivery to STARS.

However, NextGen Weather System's tilt-by-tilt and mosaic motion compensation (Figure 3-7) effectively cancels some of the latency components by advecting radar observations to a future time. Data alignments occur between the radars' end-of-tilt time to the mosaic trigger time, plus an additional time that is a configurable parameter ("additionalAdvectOffset_s"). This parameter compensates for post-mosaic-trigger latencies and the update period length; it is currently set to 25 s on MIT Lincoln Laboratory's test reference system and Raytheon's implementation of the NextGen Weather System. Consequently, for the assumed TPoG distribution architecture (Figure 3-6), 63.5 s of location latency is cancelled by NextGen Weather System's motion compensation scheme. The resulting total latency times are reduced to be comparable to or better than the 43.2-s specification for the ASR six-level weather product delivery (Table 3-1, bottom row), helping to address shortfall #1 (accuracy) for STARS precipitation depiction. (Caveat emptor: motion compensation does not work perfectly and cannot account for very rapid growth or decay.)

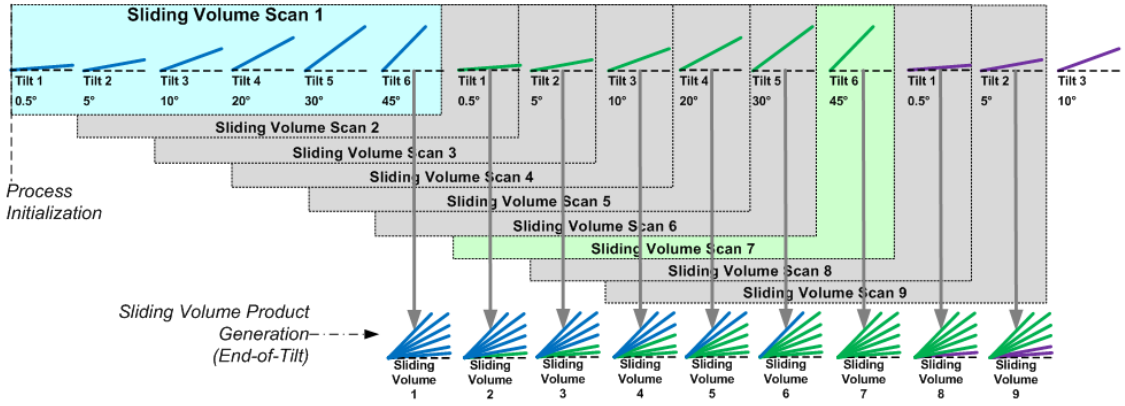

Figure 3-7. Illustration of NextGen Weather System's motion compensation scheme ("sliding volume" technique). See MIT (2019) for further information.

4. SUMMARY DISCUSSION

TPoG's concept of making precipitation display products based on a national mosaic of WX radar data available to STARS is appealing, as the quality of WX radar data is fundamentally better than that of ASR-based weather observations. This is because WX radars are specifically designed for weather surveillance, whereas the ASRs' primary mission is to detect and track aircraft. However, since WX radars are not expressly sited to cover airport and TRACON airspaces, there were questions about whether there would be acceptable coverage provided by them in all cases. Specifically, the issues in question were spatial coverage, horizontal resolution, availability rate, update period, and latency.

Our study concludes that the addition to the STARS display of a precipitation product based on a national mosaic of WX radars would, in fact, provide benefit in all of these areas, on average. Several TRACONs were identified as having especially high benefit potential for improved coverage (ASE, P50, BOI, MSO, L30, and S56), while others were flagged as potentially problematic due to lack of low-altitude coverage (EUG, MWH, ROW, CPR, and BGR). Since the FAA does not have explicitly defined requirements for 3D weather observation coverage within TRACON airspaces, we recommend further studies involving human-in-the-loop evaluations to determine what degree of coverage is acceptable for operational ATC needs.

Adding WX radars as a source for STARS precipitation depiction effectively increases the degree of coverage overlap. Even on their own, WX radars have substantial overlapping coverage, especially in regions that correspond to heavy air traffic and high hazardous weather occurrence rate (due to TDWRs being located at those types of airports). Consequently, their addition increases the aggregate data availability and the effective radar update rate at any given point in space.

The data latency analysis has more uncertainty than the other areas of study, since the future operational TPoG architecture is yet to be determined. However, based on reasonable assumptions, we project that a NextGen-Weather-System-based TPoG precipitation product would have an effective latency from start of observation to arrival at the STARS display input that is comparable to that of the current ASR-based precipitation product. This conclusion assumes that NextGen Weather System's motion compensation technique is effective in eliminating lags due to advection; it excludes situations of very rapid growth or decay in convective storms. Without taking into account motion compensation, the TPoG data latency is about twice the ASR-based latency.

Our 3D radar coverage metric, based on the WFVO formula that we developed for this study, could also be used for determining precipitation product degradation status. Because of the highly overlapping nature of the WX radar coverage, when a radar becomes unavailable, it is not obvious whether any TRACON or airport would be adversely affected by this input data dropout. The weather-weighted 3D coverage metric, which can be pre-computed for all possible combinations of radar outages for all TRACONs and airport airspaces, could then be used to declare a degradation status for any display. It would

require a determination of a threshold for the “degraded” status definition, but this can be a default value that could be customized at each site. An example of how this might work is shown in Figure 4-1. Here, over the Rochester, MN (RST) TRACON airspace, the relative 3D coverage (i.e., compared to the baseline coverage with all WX radars available) is computed for the cases when either the KARX or KMPX NEXRAD is down, and when both of those radars are down. Then, for a given threshold (96%, 94%, 90%, 85%) the table in Figure 4-1 shows which conditions would result in a “degraded” status. The status flag could be generated by the TPoG adaptor to be passed on to STARS together with the precipitation product, and/or there could be a separate web-based TPoG monitor “console” that continuously displays the relative coverage statuses of all the TRACONs, based on real-time radar availability information. We recommend a follow-up activity to develop the best approach in dealing with missing radar conditions.

Threshold	“Degraded” flag is set if…
96%	KARX or KMPX is missing
94%	KARX or KMPX is missing
90%	KARX is missing
85%	KARX and KMPX are missing

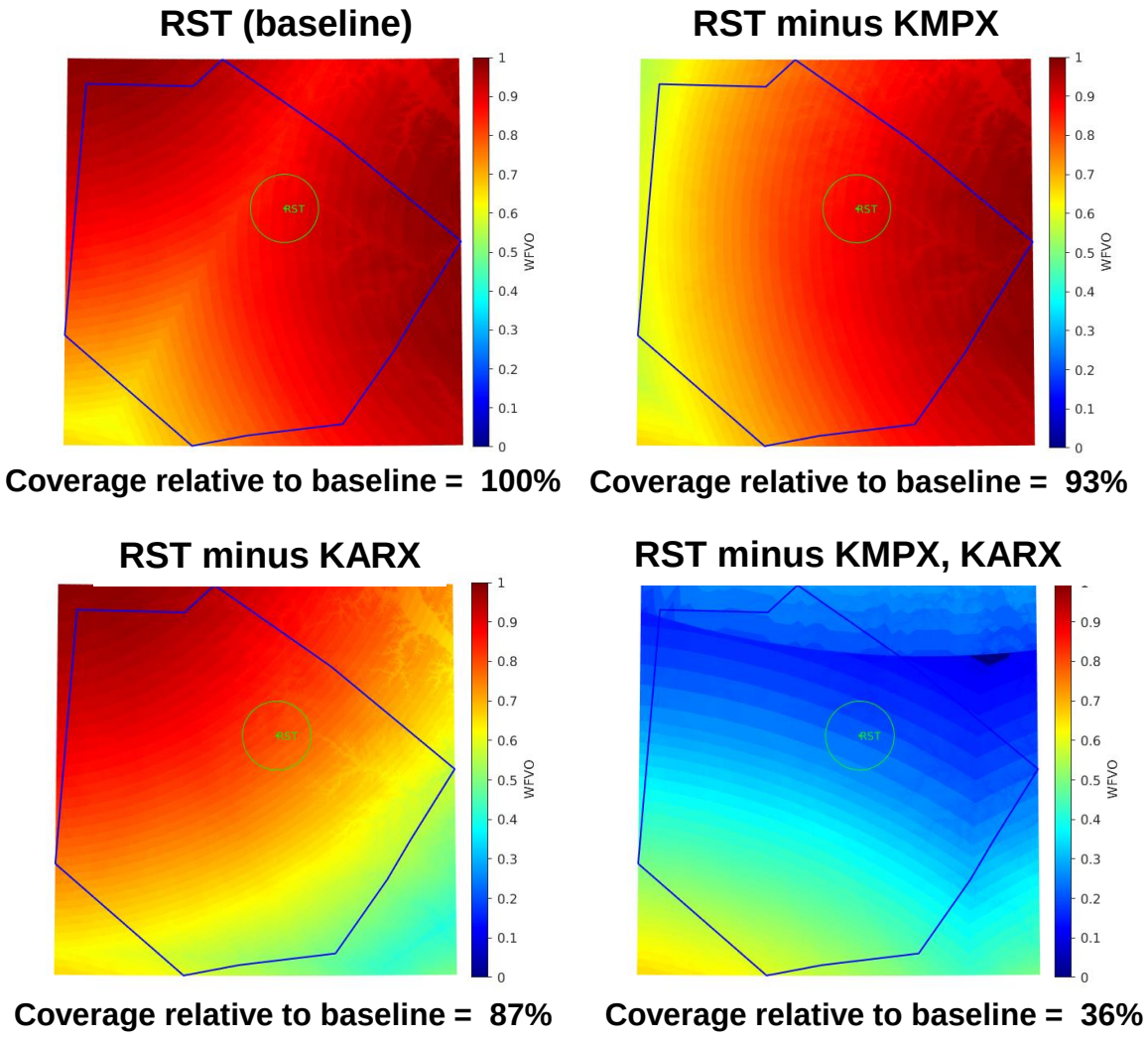

Figure 4-1. An example of using the 3D coverage metric to determine a “degraded” status for a WX-radar-based precipitation display.

This page intentionally left blank.

APPENDIX A: TABLES OF SITE-SPECIFIC PARAMETERS

Table A-1

TRACONs and Associated Airport Surveillance Radars

ID	Location	ASR-8	ASR-9	ASR-11	GPN
A11	Anchorage	ANCA		ANC	
A80	Atlanta		LZU	CSG, MCN	MGE
A90	Boston		ACK, BDL, BOS, MHT, PVD		
ABE	Allentown			ABE, AVP	
ABI	Abilene		SJT	ABI	
ABQ	Albuquerque		ABQ		
ACT	Waco			ACT	
ACY	Atlantic City		ACY, PHL		
AGS	Augusta			AGS	
ALB	Albany		ALB		
ALO	Waterloo	ALO	CID		
AMA	Amarillo			AMA	
ASE	Aspen				
AUS	Austin		AUS		
AVL	Asheville	AVL			
AVP	Wilkes-Barre			AVP	
AZA	Lansing	AZO	DTWA	MBS, MKG	MTC
AZO	Kalamazoo	AZO	DTWA	MBS, MKG	
BAD	Shreveport		BAD		
BFL	Bakersfield	BFL			
BGM	Binghamton	ELM		BGM	
BGR	Bangor			BGR	
BHM	Birmingham		BHM		
BIL	Billings			BIL	
BIS	Bismarck	BIS			
BNA	Nashville		BNA		
BOI	Boise			BOI	MUO
BTR	Baton Rouge			BTR	
BTV	Burlington			BTV	
BUF	Buffalo		BUF	ERI	
C90	Chicago		DPA, MKE, ORDA, QXM		

CAE	Columbia	GSP		AGS	SSC
CHA	Chattanooga	CHA			
CHS	Charleston, SC		CHS		SSC
CID	Cedar Rapids		CID	MLI	
CKB	Clarksburg	CKB			
CLE	Cleveland		CLE, CMH, DTWA, PIT, TOL	CAK	
CLT	Charlotte		CLT		
CMH	Port Columbus		CMH, DAY		
CMI	Champaign			CMI	
COS	Colorado Springs			COS	
CPR	Casper	CPR			
CRP	Corpus Christi		HRL	CRP	
CRW	Charleston, WV	CRW			
CVG	Cincinnati		CVG, DAY, SDF	LEX	
D01	Denver		DENA, GXY, QLO	COS	
D10	Dallas		DFWA		NFW
D21	Detroit		DTWA		
DAB	Daytona Beach		DAB, MCO	VRB	XMR
DLH	Duluth	DLH			
DSM	Des Moines		DSM		
ELM	Elmira	ELM		BGM	
ELP	El Paso		ELP		
EUG	Eugene	EUG	MFR		
EVV	Evansville	EVV			
F11	Orlando		DAB, MCO	VRB	XMR
FAI	Fairbanks			FAI	
FAR	Fargo			FAR	
FAT	Fresno			MCE	NLC
FAY	Fayetteville		RDU		FBG, GSB
FLO	Florence			MYR	FBG, SSC
FSD	Sioux Falls			FSD	
FSM	Fort Smith		FYV	FSM	
FWA	Fort Wayne		FWA		GUS
GEG	Spokane		GEG		
GGG	Longview	GGG			
GPT	Gulfport			GPT	
GRB	Green Bay			GRB	
GSO	Greensboro		GSO		

GSP	Greer	GSP			
GTF	Great Falls	GTF			
HSV	Huntsville		HSV		
HTS	Huntington	HTS			
HUF	Terre Haute	HUF			
I90	Houston		HUB, IAH	BNH, BPT, LFT	POE
ICT	Wichita		ICT		FRI
ILM	Wilmington			MYR	NCA, GSB
IND	Indianapolis		IND		
JAN	Jackson	JAN			
JAX	Jacksonville		DAB, GNV		NIP, NRB
L30	Las Vegas		LSV		
LBB	Lubbock		LBB	ABI	
LCH	Lake Charles			BPT, LFT	POE
LEX	Lexington		SDF	LEX	
LFT	Lafayette			BPT, BTR, LFT	POE
LIT	Little Rock			LIT	
M03	Memphis		MEM		
M98	Minneapolis-St. Paul		MSP		
MAF	Midland		SJT	MAF	
MCI	Kansas City		MCI		
MDT	Harrisburg		MDT	ABE, NXX	
MGM	Montgomery		MXF		
MIA	Miami		FLL		HST
MKE	Milwaukee		MKE, MSN	GRB	
MLI	Moline		CID	MLI	
MLU	Monroe	MLU			
MOB	Mobile			MOB	
MSN	Madison		MSN		VOK
MSO	Missoula		MSO		
MSY	New Orleans		MSY	LFT	
MWH	Moses Lake		MWH		
MYR	Myrtle Beach			MYR	
N90	New York		ALB, HPN, ISP, JFK, PVD, SWF	AVP	WRI
NCT	N. California		BAB, OAK	MCE, MRY, RNO, SCK	SUU
OKC	Oklahoma City		OKC		
ORF	Norfolk		RIC		NTU

P31	Pensacola			MOB, PNS	NSE
P50	Phoenix	IWA	PHX		LUF
P80	Portland, OR		PDX		
PBI	W. Palm Beach		MCO	PBI, VRB	XMR
PCT	Potomac		ADW, BWI, CHO, IAD, MDT, MRB, PHL, RIC		NHK, NYG
PHL	Philadelphia		PHL	NXX	DOV, WRI
PIT	Pittsburgh		PIT	PIA	
PSC	Pasco		PSC, YKM		
PVD	Providence		BDL, PVD		
PWM	Portland, ME		PWM, MHT		
R90	Omaha		OMA	LNK	
RDG	Reading		MDT	ABE, NXX	
RDU	Raleigh-Durham		RDU		FBG, GSB
RFD	Rockford	RFD	DPA		
ROA	Roanoke	ROA	LYH		
ROC	Rochester, NY		ROC		
ROW	Roswell		ROW		
RST	Rochester, MN			RST	
RSW	Fort Myers			RSW	
S46	Seattle		SEA		NUW
S56	Salt Lake City		SLC		
SAT	San Antonio		AUS, SATA		
SAV	Savannah				LHW, NBC
SBA	Santa Barbara			SBA, SMX	
SBN	South Bend	SBN	QXM		
SCT	S. California		BUR, LAXN, LGB, LSV, NFG, NKX, ONT, PSP		NZY
SDF	Louisville		CVG, IND, SDF	LEX	
SGF	Springfield			COU, SGF	
SUX	Sioux City			SUX	
SYR	Syracuse		ALB, SYR		
T75	St. Louis		BLV, STL	PIA, SPI	
TLH	Tallahassee	TLH			
TOL	Toledo		TOL		
TPA	Tampa		SRQ, TPA		
TRI	Tri-Cities	TRI			
TUL	Tulsa		TUL		
TYS	Knoxville		TYS		

U90	Tucson	IWA	DMA, PHX		
Y90	Bradley		BDL, HPN, PVD		
YNG	Youngstown		PIT	CAK, ERI	
BZN	Bozeman (BOI)			BOI	MUO
GJT	Grand Junction (D01)		DENA, GXY, QLO	COS, PUB	
PUB	Pueblo (D01)		DENA, GXY, QLO	COS	
MFR	Medford (EUG)	EUG	MFR		
SJT	San Angelo (MAF)		SJT	MAF	
RNO	Reno (NCT)		BAB, MCC, NUQ, OAK	MCE, MRY, RNO, SCK	SUU

Table A-2

List of TRACON-associated ASRs

ID	Location	Type	Agency
ABE	Allentown	ASR-11	FAA
ABI	Abilene	ASR-11	FAA
ABQ	Albuquerque	ASR-9 WSP	FAA
ACK	Nantucket	ASR-9	FAA
ACT	Waco	ASR-11	FAA
ACY	Atlantic City	ASR-9 WSP	FAA
ADW	Andrews AFB (Camp Springs)	ASR-9	FAA
AGS	Augusta	ASR-11	FAA
ALB	Albany	ASR-9 WSP	FAA
ALO	Waterloo	ASR-8	FAA
AMA	Amarillo	ASR-11	FAA
ANC	Anchorage-2	ASR-11	FAA
ANCA	Anchorage-1	ASR-8	FAA
AUS	Austin	ASR-9 WSP	FAA
AVL	Asheville	ASR-8	FAA
AVP	Wilkes Barre	ASR-11	FAA
AZO	Kalamazoo	ASR-8	FAA
BAB	Marysville (Beale AFB)	ASR-9	FAA
BAD	Shreveport (Barksdale AFB)	ASR-9	FAA
BDL	Windsor Locks (Bradley)	ASR-9 WSP	FAA
BFL	Bakersfield	ASR-8	FAA
BGM	Binghamton	ASR-11	FAA

BGR	Bangor	ASR-11	FAA
BHM	Birmingham	ASR-9 WSP	FAA
BIL	Billings	ASR-11	FAA
BIS	Bismarck	ASR-8	FAA
BLV	Scott AFB (Belleville)	ASR-9	FAA
BNA	Nashville	ASR-9	FAA
BNH	Brenham (CLL)	ASR-11	FAA
BOI	Boise	ASR-11	FAA
BOS	Boston	ASR-9	FAA
BPT	Beaumont	ASR-11	FAA
BTR	Baton Rouge	ASR-11	FAA
BTV	Burlington	ASR-11	FAA
BUF	Buffalo	ASR-9 WSP	FAA
BUR	Burbank	ASR-9	FAA
BWI	Baltimore	ASR-9	FAA
CAK	Akron/Canton	ASR-11	FAA
CHA	Chattanooga	ASR-8	FAA
CHO	Charlottesville	ASR-9	FAA
CHS	Charleston	ASR-9 WSP	FAA
CID	Cedar Rapids	ASR-9 WSP	FAA
CKB	Clarksburg	ASR-8	FAA
CLE	Cleveland	ASR-9	FAA
CLT	Charlotte	ASR-9	FAA
CMH	Columbus	ASR-9	FAA
CMI	Champaign	ASR-11	FAA
COS	Colorado Springs	ASR-11	FAA
COU	Columbia	ASR-11	FAA
CPR	Casper	ASR-8	FAA
CRP	Corpus Christi	ASR-11	FAA
CRW	Charleston	ASR-8	FAA
CSG	Columbus	ASR-11	FAA
CVG	Covington (Cincinnati)	ASR-9	FAA
DAB	Daytona Beach	ASR-9	FAA
DAY	Dayton	ASR-9	FAA
DENA	Denver (Irondale)	ASR-9	FAA
DFWA	West Dallas Ft. Worth	ASR-9	FAA
DLH	Duluth	ASR-8	FAA
DMA	Tucson (Davis Monthan AFB)	ASR-9 WSP	FAA

DOV	Dover	ASR-11	AF
DPA	West Chicago (DuPage)	ASR-9	FAA
DSM	Des Moines	ASR-9 WSP	FAA
DTWA	Detroit (Romulus)	ASR-9	FAA
ELM	Elmira	ASR-8	FAA
ELP	El Paso (Biggs AFB)	ASR-9 WSP	FAA
ERI	Erie	ASR-11	FAA
EUG	Eugene	ASR-8	FAA
EVV	Evansville	ASR-8	FAA
FAI	Fairbanks	ASR-11	FAA
FAR	Fargo	ASR-11	FAA
FBG	Ft. Bragg	ASR-11	Army
FLL	Ft. Lauderdale	ASR-9	FAA
FRI	Ft. Riley	ASR-11	Army
FSD	Sioux Falls	ASR-11	FAA
FSM	Ft. Smith	ASR-11	FAA
FWA	Ft. Wayne	ASR-9	FAA
FYV	Fayetteville	ASR-9	FAA
GEG	Spokane	ASR-9 WSP	FAA
GGG	Longview (Tyler)	ASR-8	FAA
GNV	Gainesville	ASR-9	FAA
GPT	Gulfport	ASR-11	FAA
GRB	Green Bay	ASR-11	FAA
GSB	Seymour Johnson AFB	ASR-11	AF
GSO	Greensboro	ASR-9	FAA
GSP	Greer (Greenville)	ASR-8	FAA
GTF	Great Falls	ASR-8	FAA
GUS	Grissom AFB	ASR-11	AF
GXY	Platteville (Denver #2)	ASR-9	FAA
HPN	White Plains	ASR-9 WSP	FAA
HRL	Harlingen (Brownsville)	ASR-9	FAA
HST	Homestead AFB	ASR-11	AF
HSV	Huntsville	ASR-9 WSP	FAA
HTS	Huntington	ASR-8	FAA
HUB	Houston (Hobby)	ASR-9	FAA
HUF	Terra Haute	ASR-8	FAA
IAD	Chantilly (Dulles)	ASR-9	FAA
IAH	Houston (International)	ASR-9	FAA

ICT	Wichita	ASR-9	FAA
IND	Indianapolis	ASR-9	FAA
ISP	Islip	ASR-9 WSP	FAA
IWA	Phoenix Mesa Gateway	ASR-8	FAA
JAN	Jackson	ASR-8	FAA
JFK	New York (Jamaica)	ASR-9	FAA
LAXN	Los Angeles (North)	ASR-9	FAA
LBB	Lubbock (Reese AFB)	ASR-9 WSP	FAA
LEX	Lexington	ASR-11	FAA
LFT	Lafayette	ASR-11	FAA
LGB	Long Beach (Garden Grove)	ASR-9	FAA
LHW	Ft. Stewart	ASR-11	Army
LIT	Little Rock	ASR-11	FAA
LNK	Lincoln	ASR-11	FAA
LSV	Nellis AFB	ASR-9	FAA
LUF	Luke AFB	ASR-11	AF
LYH	Lynchburg	ASR-9	FAA
LZU	Lawrenceville	ASR-9	FAA
MAF	Midland	ASR-11	FAA
MBS	Saginaw	ASR-11	FAA
MCE	Castle AFB (Merced)	ASR-11	FAA
MCI	Kansas City	ASR-9	FAA
MCN	Warner Robins AFB (Macon)	ASR-11	FAA
MCO	Orlando	ASR-9	FAA
MDT	Harrisburg	ASR-9 WSP	FAA
MEM	Memphis	ASR-9	FAA
MFR	Medford	ASR-9	FAA
MGE	Dobbins AFB	ASR-11	AF
MHT	Manchester (Heaton)	ASR-9	FAA
MKE	Milwaukee	ASR-9	FAA
MKG	Muskegon	ASR-11	FAA
MLI	Moline	ASR-11	FAA
MLU	Monroe	ASR-8	FAA
MOB	Mobile	ASR-11	FAA
MRB	Martinsburg	ASR-9	FAA
MRY	Monterey (Ft. Ord)	ASR-11	FAA
MSN	Madison	ASR-9 WSP	FAA
MSO	Missoula	ASR-9	FAA

MSP	Minneapolis	ASR-9	FAA
MSY	New Orleans	ASR-9	FAA
MTC	Selfridge	ASR-11	AF
MUO	Mountain Home AFB	ASR-11	AF
MWH	Moses Lake	ASR-9	FAA
MXF	Maxwell AFB (Montgomery)	ASR-9	FAA
MYR	Myrtle Beach	ASR-11	FAA
NBC	Beaufort MCAS	ASR-11	MC
NCA	New River MCAS	ASR-11	MC
NFG	Camp Pendleton MCAS (Oceanside)	ASR-9	FAA
NFW	Ft. Worth NAS	ASR-11	Navy
NHK	Patuxent River	ASR-11	Navy
NIP	Jacksonville NAS	ASR-11	Navy
NKX	Miramar MCAS (San Diego)	ASR-9	FAA
NLC	Lemoore NAS	ASR-11	Navy
NRB	Mayport NAS	ASR-11	Navy
NSE	Whiting Field NAS	ASR-11	Navy
NTU	Oceana NAS	ASR-11	Navy
NUW	Whidbey Island NAS	ASR-11	Navy
NXX	Willow Grove NAS	ASR-11	FAA
NYG	Quantico	ASR-11	MC
NZY	North Island NAS	ASR-11	Navy
OAK	Oakland	ASR-9	FAA
OKC	Oklahoma City (Will Rogers)	ASR-9	FAA
OMA	Offutt AFB (Omaha)	ASR-9	FAA
ONT	Ontario (March AFB)	ASR-9 WSP	FAA
ORDA	Chicago O'Hare #2	ASR-9	FAA
PBI	West Palm Beach	ASR-11	FAA
PDX	Portland, OR	ASR-9 WSP	FAA
PHL	Philadelphia	ASR-9	FAA
PHX	Phoenix	ASR-9	FAA
PIA	Peoria	ASR-11	FAA
PIT	Pittsburgh	ASR-9	FAA
PNS	Pensacola	ASR-11	FAA
POE	Ft. Polk AAF	ASR-11	Army
PSC	Pasco	ASR-9	FAA
PSP	Palm Springs	ASR-9	FAA
PVD	Coventry (Providence)	ASR-9	FAA

PWM	Cumberland (Portland, ME)	ASR-9	FAA
QLO	Orchard Mesa	ASR-9	FAA
QXM	Tinley Park (Chicago)	ASR-9	FAA
RDU	Raleigh-Durham	ASR-9	FAA
RFD	Rockford	ASR-8	FAA
RIC	Richmond	ASR-9 WSP	FAA
RNO	Reno	ASR-11	FAA
ROA	Roanoke	ASR-8	FAA
ROC	Rochester, NY	ASR-9 WSP	FAA
ROW	Roswell	ASR-9	FAA
RST	Rochester, MN	ASR-11	FAA
RSW	Fort Meyers	ASR-11	FAA
SATA	San Antonio	ASR-9 WSP	FAA
SBA	Santa Barbara	ASR-11	FAA
SBN	South Bend	ASR-8	FAA
SCK	Stockton	ASR-11	FAA
SDF	Louisville	ASR-9	FAA
SEA	Seattle	ASR-9 WSP	FAA
SGF	Springfield, MO	ASR-11	FAA
SJT	San Angelo	ASR-9	FAA
SLC	Salt Lake City	ASR-9	FAA
SMX	Santa Maria	ASR-11	FAA
SPI	Springfield, IL	ASR-11	FAA
SRQ	Sarasota	ASR-9 WSP	FAA
SSC	Shaw	ASR-11	AF
STL	St. Louis	ASR-9	FAA
SUU	Travis AFB	ASR-11	AF
SUX	Sioux City	ASR-11	FAA
SWF	Newburgh Stewart	ASR-9	FAA
SYR	Syracuse	ASR-9 WSP	FAA
TLH	Tallahassee	ASR-8	FAA
TOL	Toledo	ASR-9 WSP	FAA
TPA	Tampa	ASR-9	FAA
TRI	Tri City/Bristol	ASR-8	FAA
TUL	Tulsa	ASR-9	FAA
TYS	Knoxville	ASR-9 WSP	FAA
VOK	Volk Field	ASR-11	AF
VRB	Vero Beach	ASR-11	FAA

WRI	McGuire AFB	ASR-11	AF
XMR	Kennedy Space Center	ASR-11	AF
YKM	Yakima	ASR-9	FAA

Table A-3

TRACONs and Associated Remote Airport Towers

TRACON ID	Org./Facility	Tower ID	Associated Airport Towers
A11	FAA	ANC	
A11	FAA RT	MRI	Merrill Field RT
A11	FAA RT	ENA	Kenai RT
A11	Army RT off FAA	FRN	Ft. Richardson (Bryant AAF)
A11	AF RT off FAA	EDF	Elmendorf AFB RT
A80	FAA	ATL	Atlanta
A80	FAA RT	FTY	Fulton County
A80	FAA RT	PDK	DeKalb-Peachtree
A80	FAA RT	MCN	Macon
A80	FAA RT	CSG	Columbus, GA
A80	FAA RT	AHN	Athens, GA
A80	FAA RT	RYY	McCollum/Cobb County
A80	FAA RT	LZU	Gwinnet County/Briscoe
A80	Army RT off FAA	LSF	Ft. Benning/Lawson AAF
A80	AF RT off FAA	WRB	Robins AFB
A80	AF RT off FAA	MGE	Dobbins AFB
A90	FAA	BOS	Boston Logan RT
A90	FAA RT	BVY	Beverly Municipal RT
A90	FAA RT	BED	Hanscom Field/Bedford RT
A90	FAA RT	LWM	Lawrence Municipal RT
A90	FAA RT	ASH	Nashua Airport RT
A90	FAA RT	OWD	Norwood Memorial RT
A90	FAA RT	MHT	Manchester RT
A90	FAA RT	ACK	Nantucket RT
A90	FAA RT	HYA	Barnstable RT
A90	FAA RT	MVY	Martha's Vineyard RT
A90	AF RT off FAA	PSM	Pease ANGB RT
A90	CG RT off FAA	FMH	CGAS Cape Code/Falmouth RT
ABE	FAA	ABE	

ABI	FAA	ABI	
ABI	AF RT off FAA	DYS	Dyess
ABQ	FAA	ABQ	
ABQ	FAA RT	FMN	Farmington Municipal RT
ABQ	FAA RT	AEG	Double Eagle RT
ABQ	FAA RT	SAF	Santa Fe RT
ACT	FAA	ACT	
ACY	FAA	ACY	
AGS	FAA	AGS	
ALB	FAA	ALB	
ALB	FAA RT	SCH	Schenectady RT
ALO	FAA	ALO	
AMA	FAA	AMA	
ASE	FAA	ASE	
AUS	FAA	AUS	
AUS	FAA RT	GTU	Georgetown RT
AUS	FAA RT	HYI	San Marcos RT
AVL	FAA	AVL	
AVP	FAA	AVP	
AZA	FAA	LAN	Lansing
AZA	FAA RT	FNT	Flint
AZA	FAA RT	MBS	Saginaw
AZO	FAA	AZO	
AZO	FAA RT	BTL	Battle Creek RT
AZO	FAA RT	GRR	Grand Rapids
AZO	FAA RT	MKG	Muskegon
BAD	FAA	BAD	
BAD	FAA RT	DTN	Shreveport Downtown RT
BAD	FAA RT	SHV	Shreveport Regional RT
BAD	FAA RT	TXK	Texarkana RT
BAD	AF RT off FAA	BAD	Barksdale AFB RT
BFL	FAA	BFL	
BGM	FAA	BGM	
BGR	FAA	BGR	
BHM	FAA	BHM	
BIL	FAA	BIL	
BIS	FAA	BIS	
BNA	FAA	BNA	

BNA	FAA RT	MQY	Smyrna RT
BOI	FAA	BOI	
BOI	FAA RT	BZN	Bozeman RT
BTR	FAA	BTR	
BTV	FAA	BTV	
BUF	FAA	BUF	
BUF	FAA RT	IAG	Niagara Int'l RT
BUF	FAA RT	ERI	Erie
C90	FAA	ORD	O'Hare Int'l
C90	FAA RT	PWK	Palwaukee
C90	FAA RT	GYY	Gary, IN
C90	FAA RT	ARR	Aurora
C90	FAA RT	MDW	Midway Airport
C90	FAA RT	DPA	DuPage Airport
C90	FAA RT	UGN	Waukegan Regional
CAE	FAA	CAE	
CHA	FAA	CHA	
CHS	FAA	CHS	
CID	FAA	CID	
CID	FAA RT	DBQ	Dubuque RT
CKB	FAA	CKB	
CLE	FAA	CLE	
CLE	FAA RT	MFD	Mansfield
CLE	FAA RT	CAK	Akron
CLE	FAA RT	BKL	Burke-Lakefront RT
CLE	FAA RT	CGF	Cuyahoga RT
CLT	FAA	CLT	
CLT	FAA RT	JQF	Concord Regional RT
CLT	FAA RT	HKY	Hickory Regional RT
CMH	FAA	CMH	
CMH	FAA RT	OSU	Ohio State University RT
CMH	FAA RT	LCK	Rickenbacker RT
CMH	FAA RT	DAY	Dayton
CMH	AF RT off FAA	FFO	Wright Patterson AFB
CMI	FAA	CMI	
COS	FAA	COS	
COS	Army RT off FAA	FCS	Fort Carson AAF RT
COS	AF RT off FAA	AFF	Air Force Academy RT

CPR	FAA	CPR	
CRP	FAA	CRP	
CRP	FAA RT	MFE	McAllen RT
CRP	FAA RT	HRL	Harlingen Rio Grande RT
CRP	FAA RT	BRO	Brownsville RT
CRP	FAA RT	LRD	Laredo RT
CRW	FAA	CRW	
CVG	FAA	CVG	
CVG	FAA RT	LUK	Cincinnati Lunken RT
D01	FAA	DEN	Denver
D01	FAA RT	EGE	Eagle RT
D01	FAA RT	PUB	Pueblo
D01	FAA RT	FTG	Front Range
D01	FAA RT	GJT	Grand Junction
D01	FAA RT	APA	Centennial
D01	FAA RT	BJC	Jefferson Co.
D01	AF RT off FAA	BKF	Aurora-Buckley ANGB
D10	FAA	DFW	Dallas
D10	FAA RT	ADS	Addison
D10	FAA RT	AFW	Ft. Worth Alliance
D10	FAA RT	FTW	Ft. Worth Meacham
D10	FAA RT	DAL	Dallas Love Field
D10	FAA RT	RBD	Redbird
D10	FAA RT	TKI	McKinney Muni
D10	FAA RT	GPM	Grand Prairie Muni
D10	FAA RT	GKY	Arlington
D10	FAA RT	DTO	Denton
D10	FAA RT	FWS	Spinks
D21	FAA	DTW	
D21	FAA RT	ARB	Ann Arbor RT
D21	FAA RT	DET	Detroit Metro RT
D21	FAA RT	PTK	Oakland Pontiac RT
D21	FAA RT	YIP	Willow Run Tower RT
DAB	FAA	DAB	
DAB	FAA RT	OMN	Ormond Beach RT
DAB	FAA RT	EVB	New Smyrna Beach RT
DLH	FAA	DLH	
DSM	FAA	DSM	

ELM	FAA	ELM	
ELP	FAA	ELP	
ELP	Army RT off FAA	BIF	Biggs AAF RT
EUG	FAA	EUG	
EUG	FAA RT	MFR	Medford RT
EVV	FAA	EVV	
F11	FAA	MCO	Orlando
F11	FAA RT	MLB	Melbourne RT
F11	FAA RT	TIX	Titusville RT
F11	FAA RT	ORL	Orlando Exec RT
F11	FAA RT	SFB	Orlando Sanford RT
F11	FAA RT	ISM	Kissimmee RT
F11	AF RT off FAA	COF	Patrick AFB RT
FAI	FAA	FAI	
FAI	Army RT off FAA	FBK	Ft. Wainwright RT
FAI	AF RT off FAA	EIL	Eielson AFB RT
FAR	FAA	FAR	
FAT	FAA	FAT	
FAY	FAA	FAY	
FAY	Army RT off FAA	HFF	Mackall AAF RT
FAY	Army RT off FAA	FBG	Simmons AAF RT
FAY	AF RT off FAA	POB	Pope AFB RT
FLO	FAA	FLO	
FSD	FAA	FSD	
FSM	FAA	FSM	
FSM	FAA RT	ASG	Springdale Muni RT
FSM	FAA RT	FYV	Fayetteville RT
FSM	FAA RT	XNA	Northwest Arkansas RT
FWA	FAA	FWA	
GEG	FAA	GEG	
GEG	FAA RT	SFF	Felts Field RT
GEG	FAA RT	MSO	Missoula RT
GEG	AF RT off FAA	SKA	Fairchild AFB RT
GGG	FAA	GGG	
GGG	FAA RT	TYR	Tyler RT
GPT	FAA	GPT	
GPT	AF RT off FAA	BIX	Keesler AFB RT
GRB	FAA	GRB	

GRB	FAA RT	ATW	Appleton RT
GRB	FAA RT	TVC	Traverse City RT
GSO	FAA	GSO	
GSO	FAA RT	INT	Winston-Salem RT
GSP	FAA	GSP	
GSP	FAA RT	GMU	Greenville RT
GTF	FAA	GTF	
HSV	FAA	HSV	
HSV	Army RT off FAA	HUA	Redstone AAF RT
HTS	FAA	HTS	
HUF	FAA	HUF	
I90	FAA	IAH	Houston ATCT
I90	FAA RT	DWH	DW Hooks Memorial RT
I90	FAA RT	HOU	Houston Hobby RT
I90	FAA RT	BPT	Beaumont RT
I90	FAA RT	SGR	Sugarland Hull Field RT
I90	FAA RT	GLS	Galveston
I90	FAA RT	CXO	Conroe
I90	FAA RT	CLL	College Station RT
I90	AF RT off FAA	EFD	Ellington
ICT	FAA	ICT	
ICT	FAA RT	HUT	Hutchinson RT
ICT	FAA RT	SLN	Salina RT
ICT	AF RT off FAA	IAB	McConnell AFB RT
ILM	FAA	ILM	
IND	FAA	IND	
JAN	FAA	JAN	
JAN	FAA RT	HKS	Hawkins RT
JAX	FAA	JAX	
JAX	FAA RT	CRG	Craig RT
JAX	FAA RT	GNV	Gainsville RT
JAX	FAA RT	SGJ	St. Augustine RT
JAX	FAA RT	VQQ	Cecil Field RT
L30	FAA	LAS	
L30	FAA RT	VGT	North Las Vegas RT
L30	FAA RT	HND	Henderson RT
L30	FAA RT	GCN	Grand Canyon RT
LBB	FAA	LBB	

LCH	FAA	LCH	
LCH	FAA RT	CWF	Chennault RT
LEX	FAA	LEX	
LFT	FAA	LFT	
LFT	FAA RT	ARA	Acadiana RT
LIT	FAA	LIT	
LIT	AF RT off FAA	LRF	Little Rock AFB RT
M03	FAA	MEM	Memphis
M03	FAA RT	OLV	Olive Branch
M98	FAA	MSP	
M98	FAA RT	FCM	Flying Cloud
M98	FAA RT	MIC	Crystal
M98	FAA RT	STP	St. Paul Holman Field
M98	FAA RT	ANE	Anoka County
MAF	FAA	MAF	
MAF	FAA RT	SJT	San Angelo RT
MCI	FAA	MCI	
MCI	FAA RT	MKC	Kansas City Downtown RT
MCI	FAA RT	FOE	Forbes RT
MCI	FAA RT	OJC	Johnson County RT
MCI	FAA RT	TOP	Topeka
MDT	FAA	MDT	
MDT	FAA RT	CXY	Capital City RT
MDT	FAA RT	LNS	Lancaster RT
MGM	FAA	MGM	
MGM	AF RT off FAA	MXF	Maxwell AFB RT
MIA	FAA	MIA	
MIA	FAA RT	FLL	Ft. Lauderdale/Hollywood RT
MIA	FAA RT	FXE	Fort Lauderdale Exec. RT
MIA	FAA RT	HWO	North Perry Airport RT
MIA	FAA RT	OPF	Opa Locka RT
MIA	FAA RT	PMP	Pompano Beach RT
MIA	FAA RT	TMB	Tamiami Executive RT
MKE	FAA	MKE	
MKE	FAA RT	ENW	Kenosha RT
MKE	FAA RT	MWC	Lawrence J. Timmerman RT
MKE	FAA RT	UES	Waukesha RT
MKE	FAA RT	OSH	Oshkosh ATCT

MLI	FAA	MLI	
MLU	FAA	MLU	
MOB	FAA	MOB	
MOB	FAA RT	BFM	Downtown RT
MSN	FAA	MSN	
MSO	FAA	MSO	
MSY	FAA	MSY	
MSY	FAA RT	NEW	Lakefront RT
MSY	FAA RT	HUM	Houma-Terrebonne RT
MWH	FAA	MWH	
MYR	FAA	MYR	
MYR	FAA RT	CRE	Grand Strand RT
N90	FAA	JFK	Kennedy Int'l
N90	FAA RT	OXC	Waterbury Oxford
N90	FAA RT	CDW	Caldwell-Essex Co., NJ
N90	FAA RT	HPN	White Plains Westchester
N90	FAA RT	POU	Poughkeepsie Dutchess
N90	FAA RT	MMU	Morristown, NJ
N90	FAA RT	ISP	Islip Long Island
N90	FAA RT	EWR	Newark, NJ
N90	FAA RT	FRG	Farmingdale Republic
N90	FAA RT	TEB	Teterboro, NJ
N90	FAA RT	LGA	LaGuardia
N90	FAA RT	SWF	Stewart
N90	FAA RT	DXR	Danbury
N90	FAA RT	HVN	New Haven, CT
N90	FAA RT	BDR	Bridgeport
N90	AF RT off FAA	FOK	Gabreski
NCT	FAA	SFO	San Francisco
NCT	FAA RT	PAO	Palo Alto
NCT	FAA RT	APC	Napa
NCT	FAA RT	STS	Santa Rosa
NCT	FAA RT	SCK	Stockton
NCT	FAA RT	RHV	Reid Hillview San Jose
NCT	FAA RT	SAC	Sacramento Executive
NCT	FAA RT	MRY	Monterey
NCT	FAA RT	SQL	San Carlos
NCT	FAA RT	CIC	Chico

NCT	FAA RT	HWD	Hayward
NCT	FAA RT	SJC	San Jose
NCT	FAA RT	OAK	Oakland International
NCT	FAA RT	SMF	Sacramento Int'l
NCT	FAA RT	CCR	Concord Buchanan Field
NCT	FAA RT	LVK	Livermore Muni
NCT	FAA RT	SNS	Salinas Muni
NCT	FAA RT	MOD	Modesto
NCT	FAA RT	MHR	Mather
NCT	FAA RT	RNO	Reno
NCT	FAA RT	RDD	Redding
NCT	NASA RT off FAA	NUQ	NASA Ames (Moffett)
NCT	AF RT off FAA	BAB	Beale AFB
OKC	FAA	OKC	
OKC	FAA RT	OUN	Norman RT
OKC	FAA RT	PWA	Wiley Post RT
OKC	AF RT off FAA	TIK	Tinker AFB RT
ORF	FAA	ORF	
ORF	FAA RT	PHF	Newport News RT
ORF	AF RT off FAA	LFI	Langley AFB RT
ORF	AF RT off FAA	FAF	Felker RT
ORF	CG RT off FAA	ECG	Elizabeth City RT
P31	FAA	PNS	
P31	FAA RT	NPA	NAS Pensacola ATCT
P31	FAA RT	NSE	Whiting Field NAS North ATCT
P31	FAA RT	NDZ	Whiting Field NAS South ATCT
P50	FAA	PHX	
P50	FAA RT	PRC	Prescott RT
P50	FAA RT	SDL	Scottsdale RT
P50	FAA RT	FFZ	Mesa Falcon Field RT
P50	FAA RT	IWA	Williams Gateway RT
P50	FAA RT	CHD	Chandler RT
P50	FAA RT	DVT	Deer Valley RT
P80	FAA	PDX	
P80	FAA RT	HIO	Hillsboro RT
P80	FAA RT	TTD	Portland-Troutdale RT
P80	FAA RT	UAO	Aurora RT
PBI	FAA	PBI	

PBI	FAA RT	BCT	Boca Raton
PBI	FAA RT	SUA	Witham Field
PBI	FAA RT	FPR	Ft. Pierce
PBI	FAA RT	VRB	Vero Beach
PCT	FAA RT	BWI	Baltimore-Washington
PCT	FAA RT	DCA	Reagan National
PCT	FAA RT	IAD	Dulles International
PCT	FAA RT	RIC	Richmond
PCT	FAA RT	ADW	Andrews
PCT	FAA RT	CHO	Charlottesville
PCT	FAA RT	HGR	Hagerstown
PCT	FAA RT	HEF	Manassas
PCT	FAA RT	MTN	Martin State
PCT	FAA RT	ESN	Easton RT
PCT	FAA RT	JYO	Leesburg
PCT	Army RT off FAA	DAA	Ft. Belvoir/Davison AAF
PCT	AF RT off FAA	MRB	Martinsburg Air National Guard
PHL	FAA	PHL	
PHL	FAA RT	PNE	North Philadelphia RT
PHL	FAA RT	TTN	Trenton Mercer RT
PHL	FAA RT	ILG	New Castle RT
PIT	FAA	PIT	
PIT	FAA RT	AGC	Allegheny County RT
PIT	FAA RT	BVI	Beaver County RT
PSC	FAA	PSC	
PSC	FAA RT	YKM	Yakima RT
PVD	FAA	PVD	
PVD	FAA RT	GON	Groton-New London RT
PVD	FAA RT	EWB	New Bedford Regional RT
PVD	AF RT off FAA	OQU	Quonset State RT
PWM	FAA	PWM	
R90	FAA RT	OMA	Omaha Eppley Field ATCT
R90	FAA RT	LNK	Lincoln RT
R90	AF RT off FAA	OFF	Offutt AFB RT
RDG	FAA	RDG	
RDU	FAA	RDU	
RFD	FAA	RFD	
ROA	FAA	ROA	

ROA	FAA RT	LYH	Lynchburg RT
ROC	FAA	ROC	
ROW	FAA	ROW	
RST	FAA	RST	
RSW	FAA	RSW	
RSW	FAA RT	APF	Naples RT
RSW	FAA RT	FMY	Page RT
RSW	FAA RT	PGD	Punta Gorda RT
S46	FAA RT	SEA	Seattle Tacoma ATCT
S46	FAA RT	TIW	Tacoma Narrows RT
S46	FAA RT	BFI	Boeing Field RT
S46	FAA RT	OLM	Olympia Airport RT
S46	FAA RT	PAE	Paine Field RT
S46	FAA RT	RNT	Renton Municipal RT
S46	AF RT off FAA	TCM	McChord AFB RT
S56	FAA	SLC	
S56	FAA RT	OGD	Ogden-Hinckley RT
S56	FAA RT	PVU	Provo RT
S56	AF RT off FAA	HIF	Hill AFB RT
SAT	FAA	SAT	
SAT	FAA RT	SSF	Stinson Municipal RT
SAT	AF RT off FAA	SKF	Kelly AFB RT
SAT	AF RT off FAA	RND	Randolph AFB RT
SAV	FAA	SAV	
SAV	Army RT off FAA	SVN	Hunter AAF RT 1
SAV	Army RT off FAA	LHW	Wright AAF RT 1
SBA	FAA	SBA	
SBA	FAA RT	SBP	San Luis Obispo RT
SBA	FAA RT	SMX	Santa Maria RT
SBA	AF RT off FAA	VBG	Vandenberg AFB RT
SBN	FAA	SBN	
SCT	FAA	LAX	Los Angeles Int'l
SCT	FAA RT	SNA	John Wayne/Orange Co.
SCT	FAA RT	VNY	Van Nuys
SCT	FAA RT	SDM	San Diego Brown Fld
SCT	FAA RT	SMO	Santa Monica
SCT	FAA RT	TOA	Torrance
SCT	FAA RT	SEE	San Diego Gillespie

SCT	FAA RT	CNO	Chino
SCT	FAA RT	SAN	San Diego Lindberg
SCT	FAA RT	HHR	Hawthorne
SCT	FAA RT	BUR	Burbank/Glendale/Pasadena
SCT	FAA RT	RAL	Riverside
SCT	FAA RT	MYF	San Diego Montgomery
SCT	FAA RT	POC	Laverne Brackett Field
SCT	FAA RT	CRQ	Carlsbad Palomar
SCT	FAA RT	ONT	Ontario
SCT	FAA RT	EMT	El Monte
SCT	FAA RT	FUL	Fullerton
SCT	FAA RT	LGB	Long Beach
SCT	FAA RT	RNM	Ramona
SCT	FAA RT	WHP	Whiteman
SCT	FAA RT	PSP	Palm Springs
SCT	Army RT off FAA	SLI	Los Alamitos
SCT	Navy RT off FAA	NKX	Miramar MCAS
SDF	FAA	SDF	
SDF	FAA RT	LOU	Bowman Field
SGF	FAA	SGF	
SUX	FAA	SUX	
SYR	FAA	SYR	
SYR	FAA RT	RME	Rome ATCT
T75	FAA RT	STL	St. Louis ATCT
T75	FAA RT	SUS	Chesterfield Spirit of St. Louis
T75	FAA RT	ALN	Alton
T75	FAA RT	CPS	Cahokia/E. St. Louis
T75	FAA RT	PIA	Peoria
T75	FAA RT	SPI	Springfield, IL
T75	AF RT off FAA	BLV	Scott AFB
TLH	FAA	TLH	
TOL	FAA	TOL	
TPA	FAA	TPA	
TPA	FAA RT	PIE	Clearwater Int'l RT
TPA	FAA RT	SPG	Albert Whitted/St Petersburg RT
TPA	FAA RT	SRQ	Sarasota/Bradenton RT
TPA	FAA RT	LAL	Lakeland RT
TPA	AF RT off FAA	MCF	MacDill AFB RT

TRI	FAA	TRI	
TUL	FAA	TUL	
TUL	FAA RT	RVS	Tulsa RL Jones RT
TYS	FAA	TYS	
U90	FAA RT	TUS	Tucson ATCT
U90	FAA RT	RYN	Ryan Airport RT
U90	AF RT off FAA	DMA	Davis-Monthan AFB RT
Y90	AF RT off FAA	CEF	Westover ARB RT
Y90	FAA	BDL	
Y90	FAA RT	HFD	Hartford-Brainard RT
Y90	FAA RT	BAF	Barnes Municipal RT
YNG	FAA	YNG	

Table A-4

NEXRADs with Minimum Antenna Beam Elevation Angle Less Than 0.5°

ID	Location	Min. El. (deg)
KBUF	Buffalo	0.3
KCLE	Cleveland	0.4
KCLX	Grays	0.3
KDGX	Jackson	0.3
KDLH	Duluth	0.2
KFSX	Flagstaff	-0.2
KGJX	Grand Junction	-0.2
KGSP	Greer	0.2
KICX	Cedar City	0.2
KLGX	Langley Hill	0.2
KMAX	Medford	-0.2
KMBX	Deering	0.3
KMSX	Missoula	-0.2
KMTX	Salt Lake City	0
KMUX	Los Gatos	0
KRAX	Clayton	0.2
KRGX	Nixon	0
KSHV	Shreveport	0.3

Table A-5

TDWR Minimum and Maximum Antenna Beam Elevation Angles

ID	Location	Min. El. (deg)	Max. El. (deg)
ADW	Andrews AFB	0.3	42.5
ATL	Atlanta	0.3	31.1
BNA	Nashville	0.4	26.5
BOS	Boston	0.3	20.1
BWI	Baltimore	0.5	42
CLE	Cleveland	0.2	22.6
CLT	Charlotte	0.2	29.1
CMH	Columbus	0.1	29.8
CVG	Cincinnati	0.1	26.1
DAL	Dallas Love	0.5	33.7
DAY	Dayton	0.3	26.1
DCA	Washington National	0.3	37.7
DEN	Denver	0.3	24
DFW	Dallas Ft. Worth	0.4	20.1
DTW	Detroit	0.1	26.1
EWR	Newark	0.3	34.6
FLL	Ft. Lauderdale	0.3	20.1
HOU	Houston Hobby	0.2	28.4
IAD	Dulles	0.3	26.9
IAH	Houston International	0.1	20.1
ICT	Wichita	0.2	26.7
IND	Indianapolis	0.3	35.7
JFK	New York Kennedy	0.5	44
LAS	Las Vegas	0.8	29.8
MCI	Kansas City	0.3	20.1
MCO	Orlando	0.3	55
MDW	Chicago Midway	0.3	23.3
MEM	Memphis	0.3	27
MIA	Miami	0.2	21.2
MKE	Milwaukee	0.3	21.3
MSP	Minneapolis	0.3	20.1
MSY	New Orleans	0.3	38.3
OKC	Oklahoma City	0.5	28.2
ORD	Chicago O'Hare	0.3	20.1
PBI	West Palm Beach	0.1	23.8
PHL	Philadelphia	0.4	26.8
PHX	Phoenix	0.6	34.7
PIT	Pittsburgh	0.3	20.6

RDU	Raleigh Durham	0.3	27.9
SDF	Louisville	0.3	23.3
SLC	Salt Lake City	0.5	20.7
STL	St. Louis	0.3	46
TPA	Tampa	0.3	41.5
TUL	Tulsa	0.3	27.7

This page intentionally left blank.

APPENDIX B: TABLES OF RESULTS

Table B-1

3D Radar Coverage (%)

ID	TRACON Area			Airport (r < 6 NM) Area		
	ASR	WX	ASR+WX	ASR	WX	ASR+WX
A11	96.6	86.4	97.3	96.6	88.5	98.1
A80	94.8	97.1	98.4	94.6	97.5	99.2
A90	96.4	89	97.8	96.3	94.1	98.2
ABE	98.1	85.7	98.2	97.3	89.5	98.2
ABI	96.5	95.6	98.6	84.6	96.6	99.3
ABQ	95.3	95.4	97.8	85.8	84.6	99.7
ACT	97.9	92.2	98.9	73.7	92.6	98.1
ACY	98.4	95.3	98.5	99.7	98.8	99.7
AGS	97.4	93	98.1	83.8	92.7	98.2
ALB	95.8	91.7	97.1	92.3	91.7	99.3
ALO	97.8	81.4	97.9	97.4	74.7	97.4
AMA	97.6	98.6	98.7	70.8	98.1	99.5
ASE	0	83.6	83.6	0	75.7	75.7
AUS	97.5	97.9	98.7	91.1	99.4	99.8
AVL	86	91.6	94.5	81.3	87.9	98.3
AVP	94.9	88.6	96.2	81.4	88	95
AZA	97.4	89.2	99.1	90.5	92.2	97.6
AZO	97.5	95.1	98.9	89.1	96.8	98.6
BAD	97	99.7	99.7	84.1	99.2	100
BFL	92.2	89	97.3	84.7	86.9	96.8
BGM	97.9	98	98.2	95.3	95.5	99.1
BGR	93.8	71.4	94.4	83.9	62.1	95.9
BHM	87.8	94	96.5	80.8	96.4	99.4
BIL	95.4	96.3	97.4	82.7	77.2	91.2
BIS	95.9	97.8	98.2	76.7	97.6	99.4
BNA	96.1	99.3	99.3	85.1	99.8	99.8
BOI	43.5	59.7	62	47.4	52.1	60.1
BTR	98.1	82.8	99	74	84.3	97.9
BTV	92.9	95.5	96	84.2	99	99.7
BUF	95.4	92.4	96.8	89.9	94.1	98.7
C90	99.1	99.1	99.4	99.4	99.6	99.7
CAE	97	99.2	99.2	98.6	99.8	100

CHA	92.5	87	95.3	81.3	89.2	97.9
CHS	98	98.7	99.8	80.5	97.6	99.6
CID	94.5	91.5	98.4	88.2	92.6	96.9
CKB	96.3	84.9	96.9	82.4	77.9	95.8
CLE	97.1	95.8	97.6	96.3	99	99
CLT	96.5	99.1	99.2	87.5	100	100
CMH	96.1	98.5	98.8	87.2	99.9	99.9
CMI	97.9	90.6	98.8	79.1	93.2	97.2
COS	96	99.6	99.6	88.1	99.7	99.8
CPR	93.3	64.6	94.4	74.9	65.8	97.3
CRP	97.4	97.5	98.9	87.2	95.7	99.3
CRW	94.7	96.8	97.3	82.4	99.4	99.7
CVG	97.2	99.7	99.7	94.3	99.9	99.9
D01	96.2	95.5	98.6	96.5	95.6	98.7
D10	99.1	98.9	99.5	99.3	99.7	99.8
D21	96.1	99.2	99.4	93.1	99.9	99.9
DAB	99.2	89.2	99.2	99.3	87.7	99.3
DLH	94.7	98.7	98.9	78.8	84.6	95.1
DSM	97.5	98	99.1	79.2	99.7	99.9
ELM	94.8	91.1	94.9	95.5	93.5	95.5
ELP	95.2	92.4	99.3	78.1	89.1	99.6
EUG	88.8	55.8	90.5	88.4	41.6	96
EVV	96.7	96.8	98.3	81	99.6	99.6
F11	98.8	99	99.6	98.5	99.8	99.9
FAI	86.1	81.8	94.2	95.8	85.8	98.5
FAR	98.6	92.7	99.6	75.4	94.5	97.3
FAT	98.9	98	99.6	99.1	99.2	99.3
FAY	96.4	95	98.9	97	97.7	99.5
FLO	96.3	88.1	97.7	96.1	86.4	97.6
FSD	98.1	98.6	99.2	74.1	84.3	94.7
FSM	97.1	95.5	97.4	94.8	91.9	95.6
FWA	97.9	93.8	98.8	97	97.2	97.7
GEG	93.4	93.9	95.7	95.9	93.6	99.3
GGG	96.9	89.9	98.1	99.1	90.3	99.3
GPT	98.4	98.1	99.6	85.1	96.7	98.9
GRB	94.1	97.2	97.3	89.8	98.2	99.4
GSO	96.3	85.5	97	86.9	82	95
GSP	95.7	99.3	99.3	85.1	99.3	99.8

GTF	97.4	99.1	99.6	85.1	89.3	97.6
HSV	96.9	90.7	98.7	87.9	91.3	99.6
HTS	92.3	91.8	96.3	82.6	93.8	96.8
HUF	96.8	91.3	97.6	81.1	90.6	97.1
I90	97	96.7	98.9	96.3	98.6	99.7
ICT	96.2	99.5	99.5	85.9	99.9	99.9
ILM	94.7	97.9	99.4	97.2	98.6	98.9
IND	94.4	97.8	97.8	81.3	100	100
JAN	96.7	99.5	99.9	83.5	97	99.9
JAX	98.2	91.7	98.3	99.4	97.8	99.4
L30	61.4	83.2	87.3	91.3	99.4	99.6
LBB	95.9	98.9	99	73.2	97.3	99.6
LCH	95.4	99.2	99.3	95.4	99.8	100
LEX	96.3	88.5	96.8	97.4	84.5	97.4
LFT	99	87.2	99	98.9	85.9	98.9
LIT	97.5	97.1	98.6	88	97.9	99.8
M03	96.9	99.3	99.3	84.5	99.9	99.9
M98	96.3	99.2	99.3	86.6	99.6	99.7
MAF	97.5	99.1	99.3	71.9	97.5	99.5
MCI	95.6	98.7	99	90.4	98.7	98.8
MDT	96.7	79.8	97.2	92.4	73.2	98.3
MGM	96.4	96.8	99	83.9	97.5	98
MIA	98.9	99.5	99.7	98.4	100	100
MKE	95.5	94.9	97.1	93.1	99.2	99.4
MLI	98.6	98.4	99.3	84.9	99.8	99.8
MLU	97.7	84.4	98.4	76.8	78.9	97.6
MOB	98.3	99.3	99.3	86.7	99.3	99.7
MSN	98.2	93.8	99	86.1	97.1	99.5
MSO	59.6	87.1	90.9	87.7	69.2	98.6
MSY	95.2	95.4	98.1	88.7	99.5	99.6
MWH	94.5	57.2	95.1	90.1	41.1	96
MYR	98.2	95.2	99.2	89.1	99.1	99.3
N90	97.7	95.3	98.4	98.3	97.7	99
NCT	96.6	92.3	97.4	96.9	92.2	98.6
OKC	95.9	98.4	99.1	85.5	99.8	99.8
ORF	98.1	94.5	99	98.8	96.2	99.5
P31	99	93.1	99.1	99.5	91.2	99.5
P50	54.1	91.9	93.1	84.2	98	98.1

P80	88.1	91.5	94.6	91.1	89.4	95.4
PBI	98.4	99.3	99.5	93.6	99.2	99.7
PCT	97.4	92.7	97.6	98.4	97.1	99.2
PHL	99.4	98.5	99.5	99.7	99.3	99.8
PIT	95.6	99.3	99.4	91.5	99.6	99.6
PSC	88.9	78.7	93.6	90.5	66.9	96.4
PVD	94.1	95.6	96.9	92.3	98	98.5
PWM	94.1	96.4	97	85.7	98.9	99
R90	98.1	96.2	99.1	95.1	98.6	98.8
RDG	97.9	79.9	98.4	97	81.3	98.5
RDU	97.9	99.6	99.7	97.9	100	100
RFD	97	94.1	97.6	97.6	90.8	97.6
ROA	86.1	85.9	95.3	95	81.5	96.6
ROC	97.2	85.1	97.7	85.9	91.4	99.3
ROW	97.6	66.9	98.3	72	65.7	97.1
RST	97.8	86.7	98.6	76.4	87.8	96.8
RSW	98	83.2	98.7	91.9	83.4	98.9
S46	94.2	87.5	95.8	96.7	85.6	96.9
S56	78.2	91.2	93	84.2	96.7	96.8
SAT	97.4	96.9	98.1	98.6	99	99.7
SAV	98.8	97.5	99.5	98.5	98.8	99.7
SBA	87.2	89.4	94.9	92.2	90	97.5
SBN	96.8	94.3	98	81.2	96.3	97.4
SCT	95.1	79.4	96.4	97.8	79	98.6
SDF	94	98.9	99	96.1	99.7	99.7
SGF	97	97.4	97.5	76	96.1	98.7
SUX	97.8	88.5	98.7	80.9	83.6	97.9
SYR	93.2	89.2	96.8	92.6	85.5	99
T75	98.6	97	99.2	97.1	98.9	99.2
TLH	97.2	98.7	98.9	77.3	99.4	99.9
TOL	97.9	81.3	98.3	83.8	76.1	99.2
TPA	99.1	98.7	99.4	99.3	99.9	99.9
TRI	90.7	88.6	94.4	81.8	90.2	97.7
TUL	95.1	99.5	99.6	83.1	99.9	99.9
TYS	95.6	92	97.8	82.4	95.3	99.5
U90	92.4	81.8	95.1	88.2	84.3	99.3
Y90	97	91.9	97.9	99.6	84.1	99.6
YNG	92.2	91.5	97.7	94.6	92.2	96.8

Table B-2

Mean Limiting Horizontal Resolution (km)

ID	TRACON Area			Airport (r < 6 NM) Area		
	ASR	WX	ASR+WX	ASR	WX	ASR+WX
A11	1.4	1.66	1.25	0.94	1.74	0.94
A80	4.67	1.08	1.08	3	0.97	0.97
A90	4.24	1.58	1.56	3.27	1.28	1.22
ABE	3.21	2.28	2.28	2.8	2.05	2.05
ABI	4.46	1.06	1.06	2.78	0.89	0.89
ABQ	3.55	0.73	0.73	2.78	0.34	0.34
ACT	4.17	1.52	1.52	2.78	1.71	1.71
ACY	4.62	1.36	1.36	2.8	0.99	0.99
AGS	4.4	1.72	1.72	2.78	1.77	1.77
ALB	4.43	1	1	2.78	0.53	0.53
ALO	1.67	2.16	1.49	0.98	2.49	0.94
AMA	3.94	0.78	0.78	2.78	0.26	0.26
ASE	∞	2.07	2.07	∞	2.06	2.06
AUS	4.42	0.96	0.96	3.55	0.68	0.68
AVL	1.36	1.25	1.11	0.93	1.19	0.93
AVP	4.39	1.67	1.67	2.78	1.71	1.71
AZA	4.18	1.52	1.52	3.95	1.3	1.3
AZO	2.96	1.18	1.14	1.82	0.97	0.83
BAD	4.18	0.88	0.88	2.78	0.3	0.3
BFL	1.49	1.55	1.22	0.93	1.88	0.93
BGM	3.26	0.72	0.72	2.65	0.26	0.25
BGR	4.32	2.3	2.3	2.78	2.63	2.63
BHM	4.88	1.18	1.18	2.78	0.77	0.77
BIL	4.32	0.87	0.87	2.78	0.26	0.26
BIS	1.5	0.73	0.73	0.93	0.26	0.25
BNA	3.89	0.66	0.66	2.78	0.28	0.28
BOI*	∞	2	2	∞	1.82	1.81
BTR	3.9	2.31	2.31	2.78	2.25	2.25
BTV	3.9	0.75	0.75	2.78	0.26	0.26
BUF	4.41	1.58	1.58	2.78	1.1	1.1
C90	3.42	0.82	0.82	2.94	0.61	0.61
CAE	5.17	0.78	0.78	4.91	0.25	0.25
CHA	1.46	1.63	1.32	0.93	1.42	0.93

CHS	3.83	1.38	1.38	2.78	1.71	1.71
CID	4.36	1.62	1.62	5.61	1.64	1.64
CKB	1.91	2.17	1.63	0.93	2.39	0.94
CLE	4.63	1.19	1.1	3.75	0.77	0.67
CLT	4.35	1.02	1.02	2.81	0.36	0.36
CMH	4.45	0.93	0.93	2.78	0.49	0.49
CMI	4.23	1.62	1.62	2.78	1.59	1.59
COS	3.13	0.95	0.95	2.78	1.15	1.15
CPR	1.37	2.98	1.37	0.93	2.88	0.94
CRP	4.57	1.09	1.09	3.32	0.71	0.7
CRW	1.83	0.95	0.95	0.93	0.29	0.29
CVG	4.1	0.92	0.92	2.8	0.49	0.49
D01	4.27	0.92	0.92	3.22	0.52	0.52
D10	3.82	0.72	0.72	3.01	0.46	0.46
D21	4.42	0.82	0.82	3.21	0.48	0.48
DAB	3.47	1.97	1.97	2.78	2.11	2.11
DLH	1.88	0.93	0.93	0.93	0.26	0.25
DSM	4.16	0.86	0.86	2.78	0.41	0.41
ELM	1.47	1.46	1.21	0.97	1.31	0.93
ELP	3.56	0.95	0.95	2.78	0.55	0.55
EUG	2.2	2.11	1.18	1.72	2.04	0.81
EVV	1.98	1.01	1.01	0.93	0.53	0.53
F11	4	0.86	0.86	3.63	0.51	0.51
FAI	4.89	1.11	1.11	2.8	0.59	0.59
FAR	3.74	1.43	1.43	2.78	1.36	1.36
FAT	4.91	0.95	0.95	4.52	0.91	0.91
FAY	4.2	1.66	1.66	2.97	1.54	1.54
FLO	6.29	1.97	1.34	6.27	2.1	0.94
FSD	3.46	0.65	0.65	2.78	0.26	0.26
FSM	3.85	1.16	1.16	2.9	1.33	1.33
FWA	4.02	1.21	1.21	2.82	1.05	1.05
GEG	3.88	0.78	0.78	2.78	0.33	0.33
GGG	1.75	2.02	1.5	1.2	2.01	1.18
GPT	3.68	1.04	1.04	2.78	1.25	1.25
GRB	4.78	0.96	0.96	3.09	0.5	0.5
GSO	4.1	1.75	1.75	2.78	1.8	1.8
GSP	1.81	0.88	0.88	0.93	0.27	0.27
GTF	1.34	0.63	0.63	0.93	0.26	0.25

HSV	3.7	1.24	1.24	2.78	1.16	1.16
HTS	1.89	1.4	1.3	0.93	1.29	0.93
HUF	1.85	1.59	1.36	0.93	1.62	0.93
I90	4.41	1.23	1.23	3.2	0.75	0.75
ICT	4.27	0.78	0.78	3.26	0.45	0.45
ILM	5.63	1.13	1.07	5.47	1.01	0.92
IND	4.77	0.95	0.95	2.78	0.24	0.24
JAN	1.24	0.6	0.6	0.93	0.35	0.35
JAX	3.97	1.55	1.55	2.99	0.86	0.86
L30	4.84	0.79	0.79	2.82	0.41	0.41
LBB	4.26	0.85	0.85	2.78	0.26	0.26
LCH	6.41	0.77	0.77	7.12	0.27	0.27
LEX	3.87	1.7	1.7	2.82	2.02	2.02
LFT	4.06	2.01	2.01	2.8	2.16	2.16
LIT	4.5	0.94	0.94	2.78	0.29	0.29
M03	4.29	0.75	0.75	2.78	0.41	0.41
M98	4.13	0.71	0.71	2.79	0.43	0.43
MAF	3.92	0.77	0.77	2.78	0.26	0.26
MCI	4.75	0.84	0.84	4.65	0.75	0.75
MDT	4.42	2.03	2.03	3.13	2.46	2.46
MGM	4.16	1.03	1.03	2.78	1.05	1.05
MIA	3.51	0.71	0.71	2.78	0.41	0.41
MKE	5.13	1.2	1.2	3.45	0.66	0.66
MLI	3.91	0.81	0.81	2.78	0.36	0.36
MLU	1.58	2.53	1.49	0.93	2.95	0.94
MOB	3.62	0.69	0.69	2.78	0.3	0.3
MSN	3.72	1.34	1.34	2.78	1.17	1.17
MSO	3.51	0.7	0.7	2.78	0.32	0.32
MSY	5.06	1.19	1.19	3.59	0.71	0.71
MWH	3.87	2.17	2.17	2.78	2.41	2.41
MYR	4.23	1.25	1.25	2.78	0.8	0.8
N90	4.08	1.07	1.07	3.41	0.87	0.87
NCT	3.95	1.17	1.17	3.3	0.88	0.88
OKC	3.97	0.78	0.78	2.78	0.37	0.37
ORF	5.12	1.29	1.29	4.2	1.2	1.2
P31	3.48	1.57	1.57	2.78	1.78	1.78
P50	3.09	1.22	1.22	1.28	0.66	0.66
P80	3.8	0.91	0.91	2.93	0.68	0.68

PBI	3.94	0.98	0.98	3.63	0.92	0.92
PCT	3.7	1.3	1.3	3.05	0.76	0.76
PHL	3.37	0.98	0.98	2.86	0.67	0.67
PIT	3.52	0.62	0.62	2.93	0.45	0.45
PSC	3.97	1.65	1.62	2.78	2.01	1.97
PVD	4.55	1.25	1.25	3.74	0.9	0.9
PWM	4.56	0.92	0.92	2.78	0.49	0.49
R90	3.86	1.09	1.09	2.8	0.85	0.85
RDG	4.7	2.51	2.51	4.58	2.46	2.46
RDU	3.72	0.74	0.74	2.81	0.36	0.36
RFD	1.73	1.42	1.22	0.97	1.68	0.93
ROA	2.54	1.33	1.33	1.7	1.26	1.26
ROC	4.03	1.7	1.7	2.78	1.55	1.55
ROW	4.35	2.39	2.39	2.78	2.63	2.63
RST	3.99	1.91	1.91	2.78	1.85	1.85
RSW	4.34	2.29	2.29	3.35	2.28	2.28
S46	4.08	1.47	1.47	3.63	1.47	1.47
S56	4.36	0.98	0.98	3.89	0.87	0.87
SAT	4.36	1.1	1.1	2.79	0.87	0.87
SAV	3.9	1.45	1.36	3.37	1.36	1.13
SBA	3.54	0.83	0.83	2.96	0.64	0.64
SBN	1.72	1.29	1.2	0.93	1.13	0.93
SCT	3.23	1.02	1.02	2.78	0.76	0.76
SDF	4.33	0.82	0.82	2.81	0.42	0.42
SGF	4.78	0.97	0.97	2.78	0.26	0.26
SUX	3.89	1.78	1.78	2.78	2.09	2.09
SYR	5.04	1.23	1.23	3.85	1.24	1.24
T75	3.86	1.06	1.06	2.82	0.78	0.78
TLH	1.71	0.83	0.83	0.93	0.25	0.25
TOL	4.64	2.14	2.14	2.78	2.21	2.21
TPA	3.77	0.97	0.97	3.06	0.49	0.49
TRI	1.62	1.58	1.2	0.93	1.67	0.93
TUL	3.84	0.68	0.68	2.78	0.34	0.34
TYS	4.06	1.22	1.22	2.78	1.17	1.17
U90	3.8	0.92	0.92	2.79	0.82	0.82
Y90	3.94	1.61	1.61	2.82	1.98	1.98
YNG	5.84	1.58	1.58	6.33	1.56	1.56

*BOI ASR mean LHR is infinite because its associate secondary airspace, Bozeman, MT (BZN) has no ASR coverage.

Table B-3

Average Radar Coverage Overlap Count (Rounded to Nearest Integer)

ID	TRACON Area			Airport (r < 6 NM) Area		
	ASR	WX	ASR+WX	ASR	WX	ASR+WX
A11	2	1	3	2	1	3
A80	1	5	6	1	5	6
A90	2	2	3	2	2	4
ABE	2	3	4	1	3	4
ABI	1	3	5	1	3	4
ABQ	1	2	2	1	1	2
ACT	1	3	4	1	3	3
ACY	1	2	4	2	2	4
AGS	1	4	5	1	4	5
ALB	1	3	4	1	3	3
ALO	1	3	4	2	3	4
AMA	1	3	4	1	2	3
ASE	0	2	2	0	2	2
AUS	1	3	4	1	3	4
AVL	1	3	4	1	3	3
AVP	1	3	4	1	3	3
AZA	1	3	4	2	3	5
AZO	1	3	4	1	3	4
BAD	1	2	3	1	2	3
BFL	1	1	2	1	1	2
BGM	2	2	4	2	2	4
BGR	1	2	2	1	2	2
BHM	1	4	5	1	4	5
BIL	1	1	2	1	1	2
BIS	1	2	3	1	2	2
BNA	1	5	6	1	5	5
BOI	2	1	2	2	1	2
BTR	1	3	4	1	3	4
BTV	1	3	4	1	2	3
BUF	1	3	4	1	3	3

C90	3	6	9	3	6	9
CAE	2	3	5	2	3	4
CHA	1	3	4	1	3	4
CHS	1	3	4	1	2	3
CID	1	3	4	1	3	4
CKB	1	2	3	1	2	3
CLE	2	3	5	2	3	5
CLT	1	4	5	1	4	5
CMH	1	4	5	1	3	5
CMI	1	3	4	1	3	4
COS	1	3	4	1	3	3
CPR	1	1	2	1	1	2
CRP	1	2	3	1	1	2
CRW	1	2	3	1	2	3
CVG	2	4	6	2	4	6
D01	1	2	3	2	2	3
D10	2	4	6	2	4	6
D21	1	4	5	1	4	5
DAB	2	3	5	3	3	5
DLH	1	1	2	1	1	2
DSM	1	2	3	1	2	2
ELM	2	3	4	2	2	4
ELP	1	2	3	1	2	2
EUG	1	1	2	1	1	1
EVV	1	4	5	1	4	5
F11	3	3	6	3	3	6
FAI	1	1	2	1	1	2
FAR	1	2	2	1	2	2
FAT	1	2	3	2	2	4
FAY	1	3	5	2	3	5
FLO	2	4	5	2	4	6
FSD	1	2	3	1	2	2
FSM	1	3	5	2	3	5
FWA	1	3	4	2	3	5
GEG	1	1	2	1	1	2
GGG	1	2	3	1	2	3
GPT	1	3	3	1	3	3
GRB	1	2	3	1	2	3

GSO	1	3	4	1	3	3
GSP	1	3	4	1	2	3
GTF	1	1	2	1	1	2
HSV	1	4	4	1	4	4
HTS	1	3	4	1	3	3
HUF	1	4	4	1	4	4
I90	2	3	5	2	4	6
ICT	1	5	5	1	4	5
ILM	2	3	4	1	3	4
IND	1	4	5	1	4	4
JAN	1	2	3	1	2	3
JAX	2	3	5	2	3	5
L30	1	2	3	1	2	3
LBB	1	3	4	1	3	4
LCH	1	3	4	2	2	4
LEX	1	3	4	2	4	5
LFT	1	3	4	2	3	4
LIT	1	2	3	1	2	3
M03	1	3	4	1	3	4
M98	1	3	4	1	3	4
MAF	1	2	3	1	2	3
MCI	1	3	4	1	3	4
MDT	1	3	4	1	4	4
MGM	1	5	5	1	5	5
MIA	2	4	6	2	4	6
MKE	1	3	5	1	4	5
MLI	1	3	4	1	3	4
MLU	1	3	4	1	3	3
MOB	1	3	4	1	3	3
MSN	1	3	4	1	3	4
MSO	1	1	2	1	1	2
MSY	1	3	4	1	3	4
MWH	1	1	2	1	2	2
MYR	1	3	4	1	3	4
N90	3	4	6	4	4	7
NCT	2	2	4	2	2	4
OKC	1	4	5	1	4	5
ORF	1	2	4	1	2	4

P31	2	3	5	2	3	6
P50	2	2	3	3	3	4
P80	1	1	2	1	1	2
PBI	1	3	4	1	3	4
PCT	2	4	6	3	4	8
PHL	3	4	7	3	4	7
PIT	1	3	4	1	3	4
PSC	1	1	2	1	1	2
PVD	1	2	3	1	2	3
PWM	1	1	2	1	1	3
R90	2	2	4	2	2	4
RDG	3	4	6	3	3	6
RDU	2	4	6	3	4	7
RFD	1	3	5	2	4	5
ROA	1	3	4	2	3	4
ROC	1	3	4	1	3	3
ROW	1	2	3	1	2	2
RST	1	2	3	1	2	3
RSW	1	3	3	1	3	3
S46	1	2	3	1	2	3
S56	1	2	2	1	2	3
SAT	1	3	4	1	3	4
SAV	2	3	5	2	3	5
SBA	1	2	3	1	2	3
SBN	1	4	5	1	3	4
SCT	3	2	5	3	2	5
SDF	1	4	6	2	4	6
SGF	1	2	3	1	2	3
SUX	1	2	3	1	3	3
SYR	1	3	4	1	3	4
T75	2	3	5	2	3	5
TLH	1	4	5	1	3	4
TOL	1	3	4	1	4	4
TPA	2	3	5	2	3	5
TRI	1	3	4	1	3	3
TUL	1	4	5	1	4	5
TYS	1	3	3	1	2	3
U90	1	2	2	1	2	2

Y90	2	3	4	2	3	4
YNG	2	3	5	3	3	5

Table B-4

Weighted Mean WX Radar Scan Update Time (s) Averaged Over Specified Area

ID	TRACON Area	Airport (r < 6 NM) Area
A11	21.3	21.4
A80	4.7	4.7
A90	11.3	9.3
ABE	6.8	7.3
ABI	6.2	6.2
ABQ	14	15.7
ACT	7.7	7.6
ACY	9.2	8.8
AGS	5.5	5.5
ALB	7.6	8.6
ALO	8.5	7.6
AMA	8.4	10
ASE	14.1	13.7
AUS	7.3	7.3
AVL	7.9	8.4
AVP	7.3	7.6
AZA	7.2	7.1
AZO	7.1	7.5
BAD	10.2	12.3
BFL	14.5	15.6
BGM	8.6	9.9
BGR	13.9	11.4
BHM	5.4	5.4
BIL	19.4	21.2
BIS	9.9	12
BNA	4.5	4.7
BOI	16.4	15.7
BTR	6.4	6.6
BTV	8.1	10.4
BUF	7.1	8.2
C90	3.9	3.9

CAE	6.5	7.7
CHA	6.4	7
CHS	8	8.8
CID	8.5	8.1
CKB	9.7	9.7
CLE	6.9	6.4
CLT	5.6	5.7
CMH	6	6.3
CMI	6.2	6.3
COS	8.5	8.6
CPR	16	17
CRP	11.2	14.4
CRW	9.4	10.4
CVG	5.3	5.5
D01	11.4	11.4
D10	5	5
D21	5.6	5.6
DAB	7.5	7.3
DLH	17.7	21.1
DSM	12.8	14
ELM	8.4	8.8
ELP	12.5	11.3
EUG	16.3	14.5
EVV	5.4	5.4
F11	7.6	7
FAI	21.4	21.4
FAR	13.8	14.2
FAT	13.1	12.1
FAY	6.5	6.8
FLO	5.4	5.3
FSD	12.2	13.8
FSM	6.9	6.7
FWA	7	7.2
GEG	18.5	19.3
GGG	9.9	10
GPT	8.5	8.2
GRB	10	10.5
GSO	7.5	7.3

GSP	8.1	9.5
GTF	16.8	19.5
HSV	5.7	5.8
HTS	7.9	7.9
HUF	6	6.1
I90	6.3	5.8
ICT	4.7	5.1
ILM	7.5	7.7
IND	5.5	5.8
JAN	10.2	10.8
JAX	6.9	7.8
L30	11.3	10.9
LBB	6.3	6.8
LCH	8.1	8.7
LEX	6.4	5.9
LFT	7.9	8.2
LIT	10.3	11.7
M03	6.5	6.6
M98	7.4	7.6
MAF	8.6	10.6
MCI	6.6	6.7
MDT	6.6	5.8
MGM	4.7	4.7
MIA	5.9	5.6
MKE	6.1	5.8
MLI	7.9	8.2
MLU	7.2	6.7
MOB	7.5	8.4
MSN	6.6	6.6
MSO	18.8	19.7
MSY	7.3	7.4
MWH	14.7	11.5
MYR	7	7.4
N90	6.1	6.1
NCT	9.9	9.6
OKC	4.9	5
ORF	9.5	9.6
P31	6.7	6.3

P50	9.8	8.5
P80	18.7	19.8
PBI	8	8.1
PCT	6	4.8
PHL	5.9	5.9
PIT	7.6	7.9
PSC	18.2	19.2
PVD	10.4	10.9
PWM	16.9	15.7
R90	8.7	8.9
RDG	6.1	6.3
RDU	5.6	5.6
RFD	6.1	5.8
ROA	8.4	8.5
ROC	7.2	7.9
ROW	8.7	9
RST	9.3	9.7
RSW	7.4	7.2
S46	10.9	10.8
S56	12.9	12.6
SAT	7.2	7.3
SAV	7.3	7.2
SBA	12.1	12.2
SBN	6.1	6.5
SCT	9.7	10.4
SDF	4.8	4.9
SGF	8.8	10.5
SUX	9.2	8.5
SYR	7	6.8
T75	7	6.9
TLH	5.4	6.2
TOL	6.4	5.9
TPA	7.6	8
TRI	7.6	8.1
TUL	4.8	4.8
TYS	8.2	8.9
U90	12.6	11.6
Y90	7.7	7.4

YNG	7.8	7.8

This page intentionally left blank.

ACKNOWLEDGMENTS

We would like to thank: Craig Bielek (Raytheon System Engineer at the FAA Technical Center) for invaluable assistance in developing an accurate TRACON database; Kevin Hardina (System Engineer with the Regulus Group) for very helpful information on various ASR characteristics; and Greg Viola (NextGen Weather System Lead Test Director at the FAA Technical Center) for kindly providing us with measured NextGen Weather System latency data.

This page intentionally left blank.

GLOSSARY

2D	Two-Dimensional
3D	Three-Dimensional
AF	Air Force
ARSR-4	Air Route Surveillance Radar-4
ASRs	Airport Surveillance Radars
ATC	Air Traffic Control
AVSET	Automated Volume Scan Evaluation and Termination
BW	Beam Width
CANRADs	Canadian Weather Radars
CARSR	Common Air Route Surveillance Radar
CMTD	Concept Maturity and Technology Demonstration
CPI	Coherent Processing Interval
CR	Composite Reflectivity
CSS-Wx	Common Support Services Weather
FAA	Federal Aviation Administration
FVO	Fraction of Vertical Volume Observed
GPN	Ground Position Navigation
ITWS	Integrated Terminal Weather System
LHR	Limiting Horizontal Resolution
NAS	National Airspace
NEXRAD	Next Generation Weather Radar
NWP	NextGen Weather Processor
NWS	National Weather Service
SRTM	Shuttle Radar Tomography Mission
STARS	Standard Terminal Automation Replacement System
TDWRs	Terminal Doppler Weather Radars
TPoG	Terminal Precipitation on the Glass
TRACON	Terminal Radar Approach Control
VIL	Vertically Integrated Liquid
VIP	Video Integrator and Processor
VR	Virtual Radar
WFVO	Weighted Fraction of Vertical Volume Observed
WSP	Weather Systems Processor
WX	Weather

This page intentionally left blank.

REFERENCES

1. Carmouche, M., 2012: White paper: Weather products and certification in FAA long range radar systems. NAS Defense Programs, Federal Aviation Administration, Oklahoma City, OK, 12 pp.

2. Cho, J. Y. N., 2015: Revised Multifunction Phased Array Radar (MPAR) network siting analysis. Project Rep. ATC-425, MIT Lincoln Laboratory, Lexington, MA, 84 pp., https://www.ll.mit.edu/sites/default/files/publication/doc/2018-05/Cho_2015_ATC-425.pdf.

3. Cho, J. Y. N., and J. M. Kurdzo, 2019: Weather radar network benefit model for tornadoes. *J. Appl. Meteor. Climatol.*, **58**, 971-987.

4. Dupree, W., and J. Cho, 2021: Tradeoffs between NextGen Weather VIL and composite reflectivity radar products. Project Memo. 43PM-Wx-0195, MIT Lincoln Laboratory, Lexington, MA, 29 pp.

5. Chrisman, J. N., 2013: Dynamic scanning. *NEXRAD Now*, **22**, NOAA/NWS/Radar Operations Center, Norman, OK, 1–3, https://www.roc.noaa.gov/WSR88D/PublicDocs/NNOW/NNow22c.pdf.

6. Doviak, R. J., and D. S. Zrnic, 1993: *Doppler Radar and Weather Observations*. 2nd ed., Academic Press, San Diego, CA, 562 pp.

7. FAA, 1987: System requirements statement for the Terminal Doppler Weather Radar system. Order 1812.9, Federal Aviation Administration, Washington, DC, 12 pp.

8. FAA, 1995: Specification—Terminal Doppler Weather Radar with enhancements. FAA-E-2806c, Federal Aviation Administration, Washington, DC, 163 pp.

9. FAA, 2017: National airspace system capital investment plan, FY2018-2022. Federal Aviation Administration, 422 pp., https://www.faa.gov/air_traffic/publications/cip/files/FY18-22/FY18-22_CIP_Complete_Nov_2017.pdf.

10. FAA, 2008: ASR-9 system. Type FA-10064, TI6310.24, SDR-ASR9-013, William J. Hughes Technical Center, Federal Aviation Administration, Atlantic City, NJ, 464 pp.

11. FAA, 2019: ASR-11 S-band, solid state primary surveillance radar. Tech. manual SDR-ASR11-067, TI 6310.57A, Federal Aviation Administration, Washington, DC, 1579 pp.

12. FAA, 2020a: Precipitation on the Glass (PoG) preliminary shortfall analysis report. Federal Aviation Administration, Washington, DC.

13. FAA, 2020b: Solution concept of operations for Precipitation on the Glass. Federal Aviation Administration, Washington, DC.

14. FAA, 2020c: Precipitation on the Glass (PoG) alternatives. Federal Aviation Administration, Washington, DC.

15. FAA, 2021: Common Support Services-Weather (CSS-Wx) and NextGen Weather Processor (NextGen Weather System), Attachment J-07: NextGen weather systems description. Federal Aviation Administration, Washington, DC.

16. IE, 2019: Optimization for CTD on ASR-8 radars. Edition 0091, IE-UM-00830-0091, Intersoft Electronics, 214 pp.

17. Mahapatra, P. R., 1999: *Aviation Weather Surveillance Systems*. AIAA, https://doi.org/10.1049/PBRA008E.

18. Mersereau, D., 2014: This one little programming tweak will save thousands of lives. *The Vane*, http://thevane.gawker.com/this-one-little-programming-tweak-will-save-thousands-o-1592764166.

19. MIT, 2019: NextGen Weather Processor (NWP) domain technology description document. Project Rep. ATC-392, version 1.19.1, MIT Lincoln Laboratory, Lexington, MA, Project Report, 1652 pp.

20. Raytheon, 1999: Digital airport surveillance radar (DASR), contract attachment 6—system specification and SRC cross reference. Rev-D: SSG708688; cage code 49956, RFP No. F19628-95-R-0007, Raytheon Electronic Systems, Sudbury, MA, 110 pp.

21. Regulus, 2020: ASR-11 design note: Median spatial filter for weather processing. Regulus Group, 3 pp.

22. ROC, 2008: WSR-88D system specification. Document no. 2810000H, code ID 0WY55, WSR-88D Radar Operations Center, Norman, OK, 160 pp.

23. Sills, D. M. L., and P. I. Joe, 2019: From pioneers to practitioners: A short history of severe thunderstorm research and forecasting in Canada. *Atmosphere-Ocean*, **57**, 249-261, https://doi.org/10.1080/07055900.2019.1673145.

24. Skolnik, M., 2008: *Radar Handbook*, 3rd Ed. McGraw Hill, New York.

25. Torres, S. M., and C. D. Curtis, 2007: Initial implementation of super-resolution data on the NEXRAD network. *21st Int. Conf. on Interactive Information Processing Systems for Meteorology, Oceanography, and Hydrology*, Amer. Meteor. Soc., San Antonio, TX, 5B.10, https://ams.confex.com/ams/pdfpapers/116240.pdf.

26. Worris, M. A., and J. Y. N. Cho, 2018: Assessment of FAA radar precipitation weather information services for air traffic operations. Project Memo. 43PM-Wx-0177, MIT Lincoln Laboratory, Lexington, MA, 79 pp.

This page intentionally left blank.